Department of Chemical Engineering
University of Cape Town
Rondebosch 7701 South Africa

Tel +27 (0) 21 650 4091
Fax +27 (0) 21 650 5501
www.chemeng.uct.ac.za

Crystallization & Precipitation Unit

Phosphate precipitation as struvite from Municipality wastewater

This thesis is presented for the degree of

Masters in Chemical Engineering

By

Rendani Ramaru

2009

DEPARTMENT OF CHEMICAL ENGINEERING
UNIVERSITY OF CAPE TOWN

I know the meaning of plagiarism and declare that all the work in the document, save for that which is properly acknowledged, is my own

Dedication

To my late father, Martin Livhuwani Ramaru.

Acknowledgements

I give praise and thanks to you Almighty God.

I would like to thank Professor Lewis and Jeeten Nathoo for supervising this project and giving me the opportunity to further my studies in Crystallization and Precipitation research group.

Many thanks to my mom, Agnes for all her prayers and words of encouragement. To Mulugo, Mpho and Makulana for keeping it real. To my aunt, Magie Nyambeni Mudau thanks for supporting this family when things were difficult.

Special thanks to Ntsieni Mugivhi for her love, support and help through out my studies.

Many thanks to Maimela Makulana family, Raidimi family, Mulaudzi Dzivhaduhulu family and Nelushi family for their support and help.

To Mabaso Mothlatsi, Waheed Adam, Livhuwani Maake, Malivhoho Vhutshilo, Kutama Rilwele, Musenwa Lufuno and Thendo Madala . Thanks for your friendship and support.

To Miranda of the electron microscope unit (UCT), Sabine Verryn of the XRD analytical and consulting cc, Helen Divey and Lonwabo Mtebeni for their assistance with the samples analysis.

To all the members of Crystallization and Precipitation Unit (CPU). Thanks for your friendship and support. Many thanks to Thebe Mokone and Ndishavhelafhi Mbedzi for the constructive dialogues and comments through out my postgraduate studies. To Sinethemba ”Fresh” Nkukwana thanks for helping out with all the technical issues.

Many thanks to National Research Fund (NRF) for financial support. Many thanks to SSI for supplying us with the dewatering liquors.

Abstract

Tshwane Municipality produces approximately 4Ml/day of dewatering liquors arising from municipal sludge from a wastewater treatment plant. The sludge being dewatered is a combination of an anaerobically digested primary sludge and an undigested waste activated sludge. High phosphate and nitrogen are released into water during the anaerobic treatment process. High concentrations of these nutrients in the wastewater lead to eutrophication, which is a major environmental problem (Doyle et al., 2000).

In view of the above problem, the aim of this project was to investigate the feasibility of precipitating phosphate in the form of struvite ($MgNH_4PO_4.6H_2O$) from the Tshwane Municipality dewatering liquors and consequently recovering it as a valuable and marketable product.

The project was investigated in three sequential stages consisting of:

1. An aqueous thermodynamic modelling study using OLI Systems Inc. Stream Analyser Version 2.0.57 to determine the precipitation conditions required for the removal of phosphates in the dewatering liquor.
2. Bench-scale laboratory experiments to investigate the feasibility of phosphate precipitation as struvite under different pH conditions, Mg: P molar ratios and Ca:P molar ratios.
3. Fluidised bed experiments to establish the characteristics of phosphate removal at varying levels of supersaturation.

The results suggest that the pH of the system has a significant effect on phosphate removal due to its influence on the availability of PO_4^{3-}, NH_4^+ and Mg^{2+}. According to the thermodynamic modelling results, phosphates are removed as $Ca_3(PO_4)_2$ and $Mg_3(PO_4)_2.8H_2O$. Removal of phosphate as $Mg_3(PO_4)_2.8H_2O$ starts at a pH above 7 with the maximum removal achieved at pH 10. Thereafter, phosphate removal as $Mg_3(PO_4)_3.8H_2O$ drops to zero due to $Mg(OH)_2$ precipitation being favoured at the higher pH values. Thermodynamic modelling shows that a high NH_4^+:P molar ratio is required to induce struvite precipitation.

For sample C1, which had a PO_4-P and an NH_4^+ concentrations of 145mg/L and 65mg/L respectively, the bench scale experiments showed that approximately 30%, 80% and 92% of the phosphate was removed at pH 8, pH 9 and pH 10, respectively. The NH_4^+:P molar ratio in

the precipitate decreased to zero at pH 10 because NH_3 formation is favoured at this pH. The XRD analysis showed that the precipitate was $Mg_3(PO)_2.22H_2O$. On the other hand, it was shown that phosphate was removed as struvite, for sample C2, which had PO_4-P and NH_4^+ concentrations of 93mg/L and 57 mg/L, respectively. The NH_4^+: P molar ratio of sample C1 was 0.99 while the NH_4^+: P molar ratio of sample C2 was 1.35. However, it was shown that phosphate was removed as $Mg_3(PO)_2.22H_2O$ under pH 10 conditions. Thus, high NH_4^+: P molar ratios (i.e. ≥1.35) in the waste water favours struvite precipitation with the optimum pH level for phosphate removal as struvite being pH 9.

Bench scale experiments showed that, amorphous calcium phosphate precipitation is favoured over struvite precipitation at high Ca:P molar ratios. At a Ca:P molar ratio of 0.85:1, it was shown that no struvite was formed.

The bench scale experiments showed that the phosphate conversion increased at high Mg:P molar ratios. However, the effect of increasing Mg:P molar ratio on phosphate conversion was significant at pH 9. While at pH 10 there was insignificant increase of phosphate conversion as Mg:P molar ratio was increased probably due to formation of $MgOH^+$ ions at high pH levels. It was shown that high Mg:P molar ratios slightly limits calcium conversion. The calcium conversion was reduced by approximately 10% when Mg: P was increased from 1:1 to 1.4:1 for systems operated at pH 9 and pH 10 conditions. The supersaturation ratio of amorphous calcium phosphate is 10^4 greater than the magnesium compounds (i.e. struvite and $Mg_3(PO_4)_2.22H_2O$) supersaturation ratio as a result the effect of increasing Mg:P on calcium conversion was relatively very small.

The fluidized bed reactor experiments showed that high Mg:P molar ratios increased the phosphate removal as a result of the increased free Mg^{2+} concentration. However, the high Mg:P molar ratios resulted in an increased supersaturation which led to the formation of many fine particles. There was an increase in overall conversion from 68% to 83 % when the Mg:P molar ratio was increased from 1:1 to 1.2:1. On the other hand, the removal decreased from 45% to 38% when the Mg:P molar ratio was increased from 1:1 to 1.2:1. Moreover, struvite with high purity was produced at a high Mg:P molar ratios (i.e. Mg:P =1.2).

Fluidized bed reactor experiments showed that as the recycle ratio was increased the PO_4-P conversion also increased. Thus, large amount of struvite particles were recycled to the fluidized bed reactor. As a result, struvite particles provide favourable nucleation sites for struvite precipitation hence high conversion were achieved at higher recycle ratio.

Table of Contents

List of Figures

List of Tables

1. Introduction

Tshwane Municipality produces approximately 4Ml/day of dewatering liquors arising from municipal sludge from a wastewater treatment plant. The sludge being dewatered is a combination of an anaerobically digested primary sludge and an undigested waste activated sludge. High phosphates and nitrogen are released into water bodies in an anaerobic treatment process. High concentrations of these nutrients lead to eutrophication which is a major environmental problem (Doyle et al., 2000). The disposal of the sludge with high nutrients into landfills leads to long term environmental problems since the phosphorus is slowly leached to the water bodies (de-Bashan and Bashan, 2004). Therefore, it is crucial to remove both nitrogen and phosphorus from the wastewater streams to limit negative environmental impacts.

In addition, several researchers have shown that high phosphate and nitrogen concentrations in wastewater treatment plants lead to scaling due to the formation of struvite particles on the wastewater pipes (Doyle et al., 2000). Struvite scaling decreases the inner diameter of the pipes in the wastewater process, resulting in blockages, which in turn lead to increased plant maintenance and operating cost.

Several wastewater treatment techniques are used to remove phosphates on an industrial scale. These include the removal of phosphate by metal precipitation such as Fe precipitation, Al precipitation and Ca precipitation (de-Bashan and Bashan, 2004). However, the phosphorus solids produced by these methods are not recyclable due to high impurities formed. Furthermore, these methods are effective in removing the phosphate only, not the nitrogen. Shu and co-workers (2006) showed that the removal of phosphate as struvite ($MgNH_4PO_4.6H_2O$) is a better option when considering the economic benefits, given that struvite is valuable slow release fertilizer used in agriculture. The removal of the phosphate by struvite precipitation reduces the sludge handling and disposal cost. The production of fertilizer through this sustainable method is becoming increasingly attractive when considering the depletion of the limited reserves of phosphorous rocks (Shu et al., 2006; Doyle and Parsons, 2002).

Problem statement

Typical anaerobically digested wastewater streams have excess ammonium which improves the possibility of precipitating struvite. The N:P molar ratio is approximately 8:1 in the typical anaerobically digested streams (de-Bashan & Bashan, 2004). However, some wastewater

streams have relatively less ammonium concentrations compared to the phosphorus concentrations. For example, the Tshwane Municipality dewatering liquors have an NH_4^+ and PO_4-P concentrations range of approximately 57-65 mg/L and 93-145 mg/L respectively. This corresponds to the N: P molar ratio range of 1.35 – 0.99.

Objectives

The aim of this project was to investigate the feasibility of precipitating phosphate in the form of struvite ($MgNH_4PO_4.6H_2O$) from the Municipality dewatering liquors that have low ammonium concentrations thereby recovering it as a valuable and marketable product.

The first objective was to carry out a thermodynamic feasibility study. This was conducted to investigate the struvite precipitation potential under different dewatering liquor concentrations using OLI Systems Inc. Stream Analyser Version 2.0.57 (OLI Systems Inc, 2008).

The second objective was to conduct bench-scale laboratory tests to establish the feasibility of struvite precipitation under different pH conditions, Mg:P molar ratios, Ca:P molar ratios and NH_4^+:P molar ratios.

The third objective was to investigate the removal of struvite under different supersaturation levels in the fluidised bed reactor.

Thesis outline

The precipitation mechanisms that play a significant role in particle formation are discussed in detail in chapter 2, followed by struvite literature review in chapter 3. The analytical methods used and the experimental setup are presented in chapter 4. Chapter 5 presents the results and discussion followed by the conclusions and recommendations in chapter 6 and chapter 7 respectively.

2. Precipitation Theory

Precipitation is a specific form of crystallisation which is induced by chemical reaction when two chemical reagents are mixed to produce an insoluble substance. The chemical reaction results in high level of supersaturation. Hence, precipitation is also known as fast crystallisation. Due to the high levels of supersaturation and fast reaction kinetics, precipitation is mainly characterised by formation of small particles which are commonly associated with difficult solid-liquid separation characteristics (Sohnel and Garside, 1992).

2.1 Supersaturation

Supersaturation is the thermodynamic driving force for all crystallisation processes. It is defined as the ratio of the products of the activities of the dissolved ionic species to the equilibrium solubility product (K_{sp}). Thus, for the chemical reaction defined by Equation 1, the supersaturation can be expressed by Equation 2.

$$A + B \rightarrow AB \qquad \text{Equation 1}$$

$$S = \frac{a_A \cdot a_B}{K_{sp}} \qquad \text{Equation 2}$$

Where a and K_{sp} are the activity of the ionic species and the equilibrium solubility product respectively. According to Sohnel and Garside (1992), the supersaturation for an ideal solution is frequently defined as the ratio of the actual concentration in the solution to the equilibrium concentration.

$$S = \frac{C}{C_{eq}} \qquad \text{Equation 3}$$

Supersaturation is the key variable in any precipitation system. The level of supersaturation governs the rates of all processes including nucleation, crystal growth, aggregation and attrition, as shown in Figure 1.

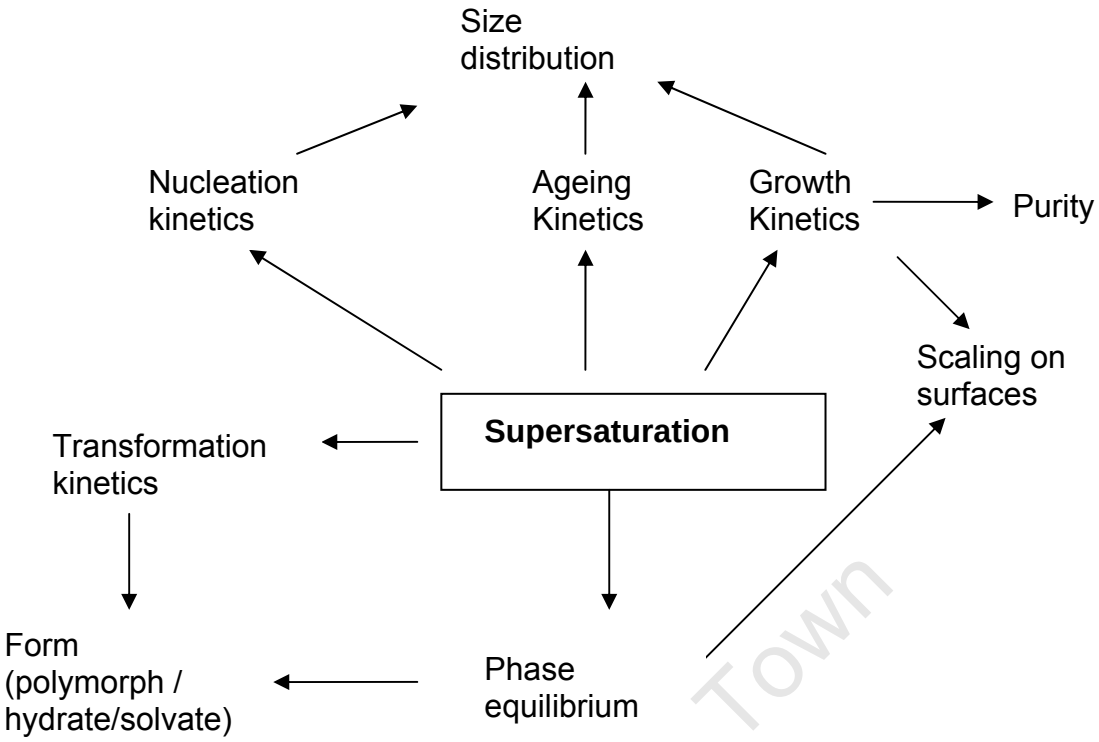

Figure 1: The role of supersaturation in precipitation process (Sohnel and Garside, 1992)

2.2 Primary particle formation mechanism

Nucleation is divided into 2 main forms i.e. primary nucleation and secondary nucleation. The former occurs mainly at higher supersaturation levels while secondary nucleation occurs at lower supersaturation and does not play a significant role in precipitation of sparingly soluble substances (Sohnel and Garside, 1992). Primary nucleation is subdivided into homogenous and heterogeneous nucleation (Jones, 2002). Homogenous nucleation is a spontaneous formation of new solid from liquid phase which requires a larger change in free energy. On the other hand, heterogeneous nucleation occurs in the presence of other foreign substances. Due to the presence of foreign particles heterogeneous nucleation occurs at a lower supersaturation because the foreign particles reduce the energy barrier for forming the critical nucleus. Hence, the change in free energy is smaller in heterogeneous nucleation compared to homogeneous nucleation. Homogenous nucleation dominates at high supersaturation levels and thus large quantity of small particles are formed which leads to filtration problems (Sohnel and Garside, 1992). The effect of supersaturation on the amount of fines formed is summarised in Figure 2.

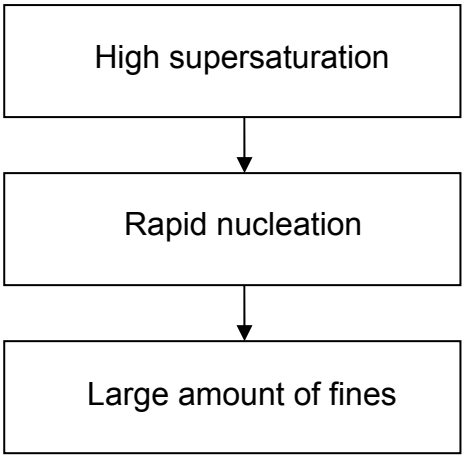

Figure 2: The effect of supersaturation on fines formation

A summary of the primary particle formation mechanisms dominating at different levels of supersaturations are shown in Figure 3. It is desirable to operate in region 2 and region 3 because a reduction in the amount of fines in the system and formation of large particles is favoured. This region is known as the metastable region.

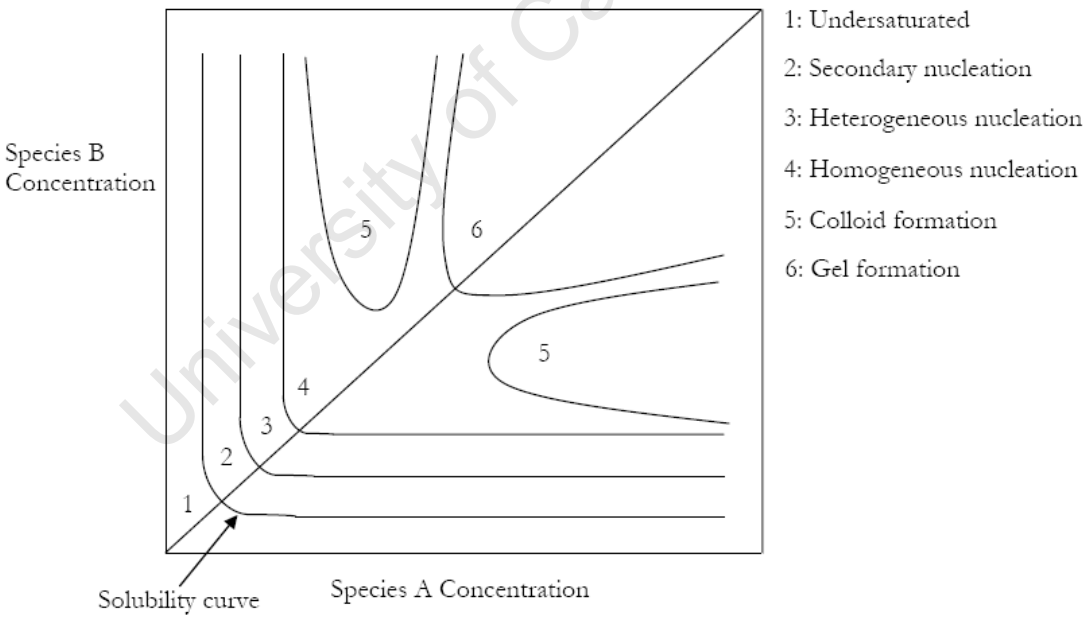

Figure 3: Associated dominant mechanism at different supersaturation level (Nielsen, 1979)

2.3 Secondary particle formation mechanism

When the primary fine particles are produced during a precipitation process they tend to grow into larger particles through particle aggregation. During aggregation fine

particles are attracted to each other. This leads to a reduction in the number of particles in the system and an increase in the average particle size. This mechanism is favoured when the inter-particle distance is smaller than 20 particle diameters (Karpinski, 2002). Thus, aggregation is enhanced in systems containing many small particles.

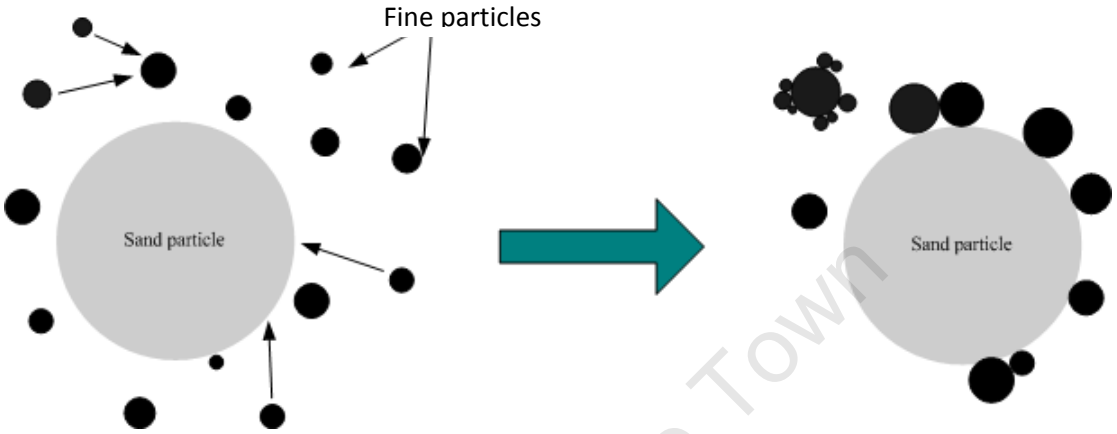

Figure 4: Aggregation of fines in the system

In contrast, attrition leads to an increase in the number of particles and decreases the average size of particle. Attrition is caused by collisions that lead to particle breakage. This mechanism dominates in the systems with high shear rates but is also dependent on the relative strength of the particles to withstand the force of impact.

3. Literature Review

The production of struvite ($MgNH_4PO_4.6H_2O$), also known as MAP, from wastewater and its use as a slow release fertiliser becomes increasingly attractive when considering the limited reserves of phosphorous rocks. This, coupled with the negative effects of struvite scaling in wastewater pipes has resulted in struvite precipitation gaining increased attention in wastewater treatment (Doyle and Parsons, 2002). A significant amount of research is currently being conducted to investigate struvite precipitation processes that will lead to product recovery and reduction in operating and maintenance costs in wastewater treatment plants.

3.1 Struvite Solubility

The solubility product of struvite is given by Equation 4 below:

$$Ksp = -\log\left[Mg^{2+}\right]\cdot\left[PO^{4-}\right]\cdot\left[NH_4^{+}\right] \qquad \text{Equation 4}$$

Struvite precipitation can only occur when the activity product of the ions in the solution exceeds the solubility product (i.e. Ksp). Ohlinger and co-workers (1998) reported the solubility product for struvite to be 10-13.26. However, various literature sources reported the solubility product to be between 10-12.6 and 10-13.26. The difference in these values is due to an ionic strength correction, as well as the formation of magnesium phosphate complexes i.e. MgH2PO4+ and MgPO4-. These complexes are included in the Minteq thermodynamic model (Ohlinger et al., 1998). The supersaturation of struvite is affected by the concentrations of Mg2+, PO43- and NH4+ in the solution. It was shown by Ali (2007) that the growth rate of crystals at different levels of supersaturation differs significantly. The growth rate of 1.625µm h-1 and 0.83µm h-1 is obtained when the supersaturation is 0.23 and 0.17 respectively (Ali, 2007). However, high supersaturations lead to the formation of fine particles through homogeneous nucleation. Therefore, supersaturation control is the most significant factor in struvite precipitation and it is highly dependent on the pH of the solution. It is therefore necessary to operate in the more stable region known as the metastable zone in order to limit rapid nucleation. The metastable region is a region between the equilibrium solubility line and point of spontaneous formation of the solid phase. At this region heterogeneous nucleation or secondary nucleation occurs while homogenous nucleation is limited (Sohnel and Garside, 1992).

In the work by Ali and co-workers (2006) the lines of Mg2+, NH4+ and PO4-P concentrations limits which induced rapid nucleation (i.e. the labile supersaturation zone) was found to be parallel to the solubility of struvite (Ali and Schneider, 2006)

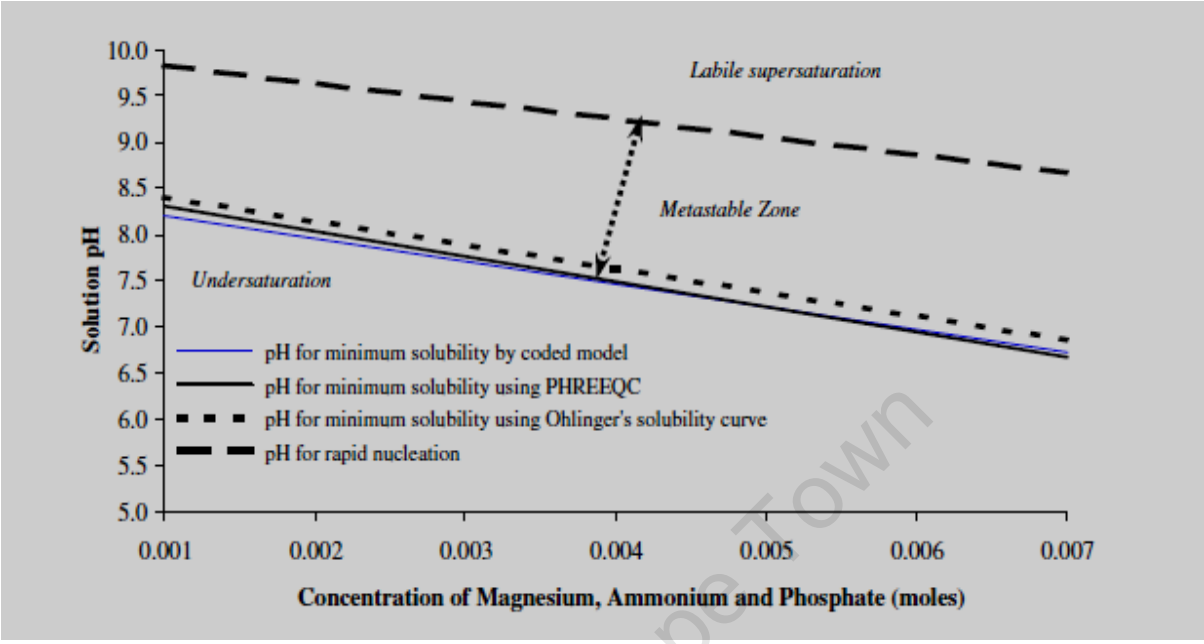

Figure 5: Metastable zone of struvite for struvite precipitation (Ali and Schneider, 2006)

3.2 The effect of pH on struvite formation

The pH indirectly influences the solubility of struvite by changing the activity of the free NH_4^+, Mg^{2+} and PO_4^{3-} ions available in the solution. An increase in pH results in a decrease in NH_4^+ ion concentration due to the formation of volatile ammonia in a proton deficient environment. This reduces struvite formation. According to Ali (2007), NH_4^+ exists as a free ion at pH below 8.5 and it forms volatile NH_3 at higher pH levels as shown in Figure 6.

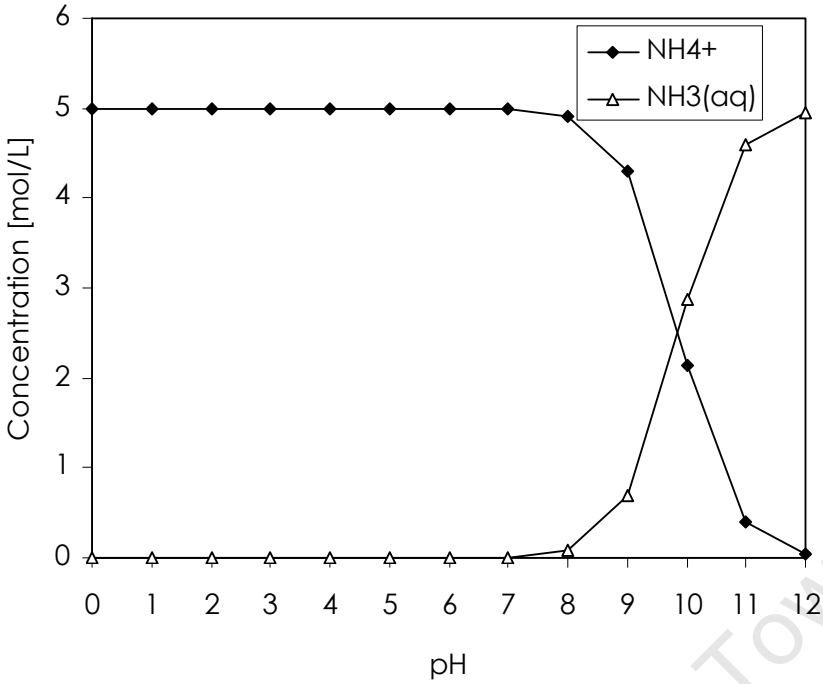

Figure 6: Typical pH dependent speciation of ammonium complexes (OLI Systems Inc, 2008)

The presence of free Mg^{2+} in solution also decreases with an increase in pH because of the formation of the $MgOH^{+}$ complex at pH level above 10.5 (Ali, 2007)

Phosphate is usually present as $MgPO_4^-$, $MgHPO_4(aq)$, $MgH_2PO_4^{2-}$,$H_2PO_4^-$, H_3PO_4 and HPO_4^{2-} at low pH levels. An increase in pH increases the availability of PO_4^{3-} ions resulting in increased struvite formation (Ali and Schneider, 2006; Doyle and Parsons, 2002). This is explained by the fact that the de-protonation of HPO^{2-}, $H_2PO_4^-$ and H_3PO_4 species are favoured at higher pH levels as shown in Equation 5. Hence, the availability of free PO_4^{3-} increases with an increase in pH as shown in Figure 7, which leads to an increase in supersaturation (Seckler et al., 1996)

$$H_3PO_4 \leftrightarrow H_2PO_4^- \leftrightarrow HPO_4^{2-} \leftrightarrow PO_4^{3-} \qquad \text{Equation 5}$$

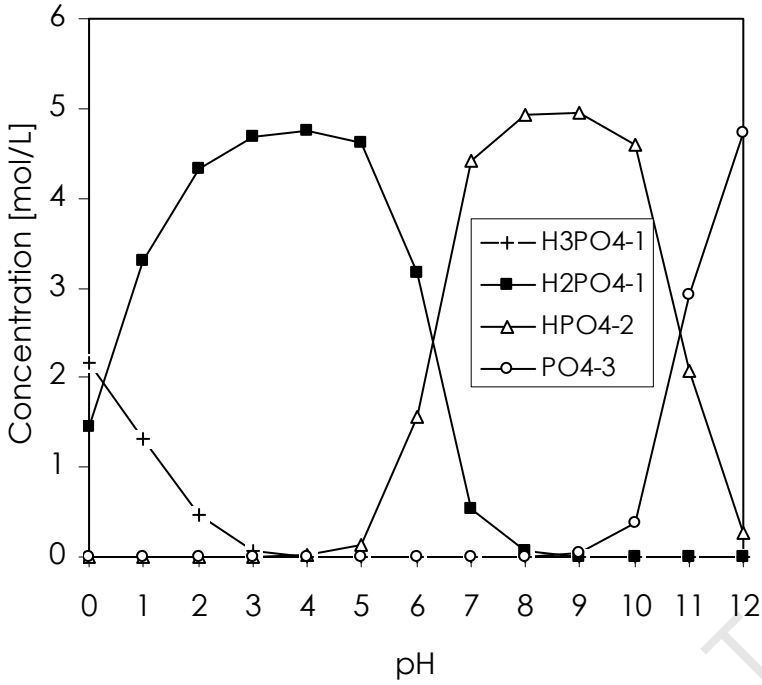

Figure 7: Typical pH dependent speciation of phosphate complexes (OLI Systems Inc, 2008)

As a result of the two counteracting effects between NH_4^+ and PO_4^{3-}, there is an optimal pH range for maximising struvite formation. Jaffer and co-workers (2001) noted that struvite formation occurs at a pH levels above 8.5 whilst dissolution of struvite occurs at the lower pH levels. On the other hand, Doyle and co-workers (2002) found that struvite precipitation is induced at a pH of 7.6 with the lowest struvite solubility occurring at a pH of 9 (Doyle and Parsons, 2002). However, Ohlinger and co-workers (1998) reported the lowest struvite solubility to be at a pH of 10.3. In summary, struvite formation occurs within a pH range of 7 to 11 depending on the composition of the stream.

3.3 The effect of Mg^{2+} ions on the formation of struvite

Possible magnesium phosphate species that are formed in the presence of Mg^{2+}, NH_4^+ and PO_4^{3-} are struvite, magnesium hydrogen phosphate ($MgHPO_4.3H_2O$ also known as newberrite) and bobietite ($Mg_3(PO_4)_2.8H_2O$) (Çelen et al., 2007). Le Corre and co-workers (2007) showed that $Mg_3(PO_4)_2.22H_2O$ precipitation is also possible (Le Corre et al., 2007). The formation of struvite is dependent on the concentration ratio of the Mg^{2+}, NH_4^+ and PO_4^3. Struvite precipitation occurs when the molar ratio of Mg^{2+}:NH_4^+:PO_4^{3-} is greater than 1:1:1 with respect to PO_4^3 concentration. Several researchers reported on the advantages of adding additional Mg^{2+} ions to the wastewater streams, wherein the Mg^{2+} concentration is usually less than the NH_4^+ and PO_4^{3-} concentrations. Le Corre and co-workers (2005) found

that better struvite crystal characteristics are obtained at higher Mg^{2+} concentrations. Nelson and co-workers (2003) found that a higher PO_4^{3-} conversion is achieved when the Mg^{2+}:PO_4^{3-} ratio is increased and showed that approximately 96% of 55mg/l of PO_4^{3-} in an untreated swine liquid is removed when the Mg^{2+}:PO_4^{3-} ratio is 1.6:1. Conversely, the effluent stream contained 10mg/l of PO_4^{3-} when the ratio of Mg^{2+}:PO_4^{3-} was 1:1. The increased conversion as a result of a higher Mg^{2+}:PO_4^{3-} molar ratio can also be used to increase the conversion at lower pH levels (Nelson et al., 2003). This could lead to significant cost benefits due to the lower alkali input requirement to achieve the same level of conversion when compared to operating at the higher pH levels.

On the other hand, Babic-Ivancic and co-workers (2006) found that newberyite formation is favoured in a system with excess Mg^{2+} concentrations and low NH_4^+ and PO_4^{3-} concentrations at pH below 7. The presence of both struvite and newberyite were apparent in the precipitated solids in the system with low ammonium and phosphate concentrations. Struvite is more abundant in the system with high ammonium and phosphate concentrations compared to Mg^{2+} concentrations. Furthermore, it was observed that, struvite completely transformed to newberyite via dissolution within 400 min resulting in larger newberyite crystals. The transformation of struvite to newberyite was found to be dependent on the ratio of the supersaturation of struvite and newberyite. In addition, it was shown that an increase in pH from 6.58 to 8.77 reduces the struvite content in the precipitated solids from 95% to 45% respectively (Babić-Ivančić et al., 2006).

A high Mg:P molar ratio increases the phosphate conversion but it limits struvite precipitation and induces precipitation of other magnesium phosphate compounds e.g. bobietite ($Mg_3(PO_4)_2.8H_2O$). Warmadewanthi and Liu (2008) showed that phosphate removal increases from 47.4% to 92% when Mg: P is increased from 1:1 to 3:1. However, it was shown that phosphate is mainly removed as bobietite ($Mg_3(PO_4)_2.8H_2O$) when the Mg: P is above 2:1 (Warmadewanthi and Liu., 2008)

$MgCl_2.6H_2O$, $Mg(OH)_2$ and MgO are the most commonly used magnesium sources. A study conducted by Uludag-Demirer and co-workers (2005) showed that, when using $Mg(OH)_2$ as the magnesium source, the pH increases up to 10. As a result, the pH and magnesium dosage are interlinked and hence cannot be controlled independently when using $Mg(OH)_2$, which would have a detrimental effect on the overall conversion at elevated pH levels above the optimal range (Uludag-Demirer et al., 2005).

On the other hand, $MgCl_2.6H_2O$ is more soluble compared to $Mg(OH)_2$ and thus results in a reduced reaction time (Uludag-Demirer et al., 2005). Moreover, $MgCl_2.6H_2O$ has no significant effect on the pH. Hence, Mg^{2+} concentration can be controlled independently of the pH. However, $MgCl_2.6H_2O$ is very expensive compared to MgO and $Mg(OH)_2$.

An alternative Mg^{2+} source includes the use of sea water, bittern (salt produced by evaporation of seawater) and low grade MgO. Bittern is effective for phosphate removal but not effective in NH_4^+ removal (Lee et al., 2003).

3.4 The effect of the presence of other ions on struvite precipitation

The presence of other ions in wastewater streams has varied effects on the extent of phosphate precipitation and the purity of struvite formed. For example, the presence of Ca^{2+} reduces the availability of PO_4^{3-} due to the formation of calcium phosphate complexes such as $CaHPO_4$, $CaH2PO_4^+$, $CaOH^+$ and $CaPO_4^-$ (Ali, 2007) and as a result struvite precipitation is affected. According to Le Corre and co-workers (2005), a high calcium concentration reduces the particle size and negatively affects the purity of the final product due to the formation of an amorphous compound. Furthermore, the presence of the calcium ions increases the struvite induction time because high calcium concentrations inhibit struvite formation (Le Corre et al., 2005).

Musvoto and co-workers (2000) suggested that, in the presence of calcium ions, the magnesium to calcium ratio should be greater than 0.6 in order to minimise the formation of calcium phosphate (Musvoto et al., 2000). Amorphous calcium phosphate (ACP) precipitation increases with an increase in pH but it is shown that only trace amounts of ACP are usually formed in anaerobic digester liquors. The ACP precipitation at a pH less than 8.5 is slower than struvite precipitation (Van Rensburg et al., 2003).

Ryu and co-workers (2007) also showed that the presence of fluoride in the wastewater inhibits the struvite precipitation. It was observed that, at a fluoride concentration of less than 592 mg/L, a PO_4^{3-} conversion of over 80% is achieved. However, a fluoride concentration over 600 mg/L reduces struvite precipitation because fluoride reacts with free Mg^{2+} (Ryu et al., 2007).

In summary, the presence of other ions limits struvite precipitation because of the side reactions which reduce the availability of free Mg^{2+}, PO_4^{3-} and NH_4^+ in solution.

3.5 Effect of excess ammonium on struvite precipitation

Several researchers have shown that struvite formation is enhanced at high NH_4^+:PO_4^{3-} molar ratios in waste water, which also improves the purity of the struvite crystals (Ryu et al., 2007 ;Stratful et al., 2001; Warmadewanthi and Liu., 2008). This is explained by the fact that NH_4^+ transportation to the crystal is increased when NH_4^+ concentration is increased (Ryu et al., 2007).

Moreover, NH_4^+ also acts as buffer of a system, hence a system with high NH_4^+ suppresses changes in the pH (Stratful et al., 2001). This effect is significant in a system that contains low concentrations of PO_4^{3-} because of the low release of protons due to the small amount of struvite precipitated. This could lead to significant cost benefits due to the lower alkali input requirements for adjusting the pH of the system. However, it is worth noting that excess NH_4^+ does not solve the environmental problems since the remaining NH_4^+ also contributes to eutrophication.

Uludag-Demirer and Othman (2009) showed that the removal rate of Mg^{2+}, $NH4^+$ and PO_4^{3-} is highly dependent on the initial molar ratios of these ions in the system. For example, low NH_4 removal (42%) and high PO_4^{3-} removal (90%) is achieved in the system with a NH_4:PO_4 molar ratio of 8.6:1, respectively. This was expected since NH_4^+ removal is mainly due to struvite formation rather than NH_3 volatilization; hence PO_4^{3-} was the limiting reactant. On the other hand, it was shown that an initial molar ratio of 1:1 for NH_4:PO_4 is preferred since high PO_4 and NH_4 removal (approximately 94% and 92%, respectively) is achieved and high purity struvite is formed (Uludag-Demirer and Othman., 2009). Thus, equimolar ratio of NH_4:PO_4 is preferable because both PO_4^{3-} and NH_4^+ are removed through struvite precipitation. This can be improved by increasing Mg^{2+} concentration in the system.

3.6 The effect of seeding on the formation of struvite

Due to the very low solubility of struvite, the supersaturation produced can be very high, resulting in the formation of small particles through primary homogeneous nucleation. Thus, the system can be operated at low supersaturations to minimize homogeneous nucleation and promote particle formation through heterogeneous nucleation. As a result, seeds can be used to lower the activation energy required for the precipitation. This allows for formation of particles with better handling characteristics.

Ali and co-workers (2006) evaluated the use of quartz sand and struvite particles in batch experiments as potential seeding materials and found that the struvite seeds proved to be more effective in enhancing struvite growth, probably due to similarities in the lattice

structure. SEM images of the quartz sand particles showed that the struvite crystals were not growing on the surface but rather, homogenous nucleation was the dominant particle formation mechanism. Moreover, 1.2 mm seed particles are preferred over 2 mm particles because the specific surface area is large and thus heterogeneous nucleation is promoted (Hirasawa et al., 2008).

Yoshino and co-workers (2003) showed that, when the mass concentration of struvite particles in the draft tube is between 10-25 %, the residence time required for 92% PO_4^{3-} conversion decreases to 4 minutes. However, when a struvite mass concentration is between 5%-10%, the kinetics of the system are very slow. Therefore, the use of a large amount of struvite particles as seed material enhances struvite precipitation (Yoshino et al., 2003). Kim and co-workers (2007) also observed that struvite particles have a significant effect on the removal of NH_4-N in municipal landfill leachate (Kim et al., 2007).

Liu and co-workers (2008) also found that struvite seeding enhanced struvite removal. However, it was observed in their work that seeding enhancement is greater for the waste water stream which has low phosphate and ammonium concentrations. 19% enhancement is achieved when the PO_4^{3-}-P and NH_4^{+}-N concentrations are 21.7mg/L and 40mg/L, respectively. On the other hand, 1% enhancement is achieved when the PO_4^{3-}-P and NH_4^{+}-N concentrations are 153mg/L and 4560mg/L, respectively. Thus, seeding enhancement is significant in the stream that has low phosphate and ammonium concentrations (Liu et al., 2008).

3.7 Zeta Potential

Several researchers showed that the zeta potential of the struvite particle becomes more negative with an increase in pH (Le Corre et al., 2007; Bouropoulos, Koutsoukos, 2000). As a result, the electrostatic repulsion increases, which limits agglomeration of the struvite particles. Consequently, the particles formed at high pH level had a small average particle size (Le Corre et al., 2007). The presence of other precipitates such as $Mg_3(PO_4)_2.8H_2O$ also had an effect on the zeta potential. For example, Warmadewanthi and Liu (2008) observed that zeta potential becomes more positive when the Mg: P molar ratio is increased due to formation of $Mg_3 (PO_4)_2.8H_2O$.

3.8 Struvite precipitation kinetics

Nelson and co-workers (2003) suggested that struvite precipitation kinetics follow a 1^{st} order kinetic model. The 1^{st} order rate constant increases from 3.7 to 12.3 for a pH increase from 8.4 to 9. On the other hand, Turker and co-workers (2007) reported that struvite nucleation fits second order kinetic model (Türker and Çelen, 2007).

Uludag-Demirer and Othman (2009) showed that the struvite follows a 3^{rd} order kinetic model if the reaction order rate is calculated in terms of Mg^{2+} conversion. On the other hand, the reaction rate order follows 1^{st} order based on PO_4^{3-} conversion. Mg^{2+} and PO_4^{3-} forms other complex compounds such as newberyite ($MgHPO_4$), bobierritte ($Mg_3(PO_4)_2.6H_2O$) etc, as a result the conversion of Mg^{2+} and PO_4^{3-} are different. NH_4^+ conversion is mainly via 2 mechanisms namely struvite precipitation and NH_3 volatilization. It was shown that NH_3 volatilization mechanism is not significant at pH 9 values. Hence, struvite kinetics can be calculated based on the NH_4^+ removal. It was shown that struvite reaction order fits all the kinetic models very well if the calculation is based on NH_4^+ removal i.e. 1^{st},2^{nd} and 3^{rd} order kinetic model with R^2 values of 0.91, 0.92 and 0.93 respectively (Uludag-Demirer and Othman, 2009).

3.9 The effect of residence time on struvite precipitation

Previous work reveals that struvite precipitation is extremely fast (Stratful et al., 2001; Yoshino et al., 2003; Lee et al., 2003). Therefore, increasing the residence time does not play any significant role in phosphate removal. Stratful et al. (2001) and Yoshino et al. (2003) found that 87% and 92% of phosphate removal is achieved within 1 minute and 4 minutes respectively. A further increase in residence time resulted in a small increase in phosphate removal. However, the residence time has a significant effect on the average particle size. Stratful and co-workers (2001) showed that the struvite crystal length increases from 0.1mm to 3mm if the residence time is increased from 1min to 180min. Moreover, Yoshino and co-workers (2003) reported that crystal diameter increases to 0.6mm if the residence time is increased to 18 hours.

3.10 The effect of mixing on struvite precipitation

Doyle and co-workers (2000) found that high turbulent mixing conditions increased the pH level, which in turn resulted in a higher struvite precipitation rate. It was observed that, stirring a 1 litre solution at 300 rpm for 100 minutes increased the pH of the wastewater from 7.2 to 8.4 (Doyle et al., 2000).

3.11 The effect of temperature on struvite formation

Mijangos and co-workers (2004) found that an increase in temperature decreases the struvite yield, suggesting that an ambient operating temperature can be used for a struvite precipitation process (Mijangos et al., 2004).

3.12 Drying struvite particles

The method used to dry the particles is a crucial aspect since transformation of struvite in to other compounds such as bobietite ($Mg_3(PO_4)_2.8H_2O$) is significant at high temperatures. In the work by Ali (2007) it was observed that the NH_4^+ and H_2O losses were extremely high at high temperatures. Consequently, the struvite structure changes and fragile particles are formed. The recommended drying temperature is between 40 and 50 ^oC which results in smaller NH_4^+ and H_2O losses (Ali, 2007).

3.13 Fluidized bed reactor (FBR) technology

A fluidized bed reactor (FBR) is reactor packed with seed particles in which the fluid is pumped from the bottom of the reactor. When the upward velocity is increased the particles separate from one another offering less resistance to the flow of fluid. The particles start to behave like a fluid when the force of the fluid is greater than the particle weight. This phenomenon is known as fluidization. As the velocity is increased the pressure difference along the bed decreases because of an increase in voidage (Richardson et al, 2002). At the point of fluidization and beyond, the system is well agitated, thus minimising the radial and axial concentration gradients. Furthermore, the presence of particles promotes heterogeneous nucleation, provided that the system is within the metastable zone. Several workers have used the fluidized bed reactor technology to treat municipal wastewater streams. For example, Battistoni et al. (2002) used a fluidized bed reactor to remove phosphate from an anaerobically digested waste sludge as $Ca_5(PO_4)_3OH$ (HAP). Seckler and co-workers (1996) used a fluidized bed reactor to remove phosphate as amorphous calcium phosphate (ACP). The fluidized bed reactor technology is also applied in the removal of heavy metals from wastewater. For example, Costodes and Lewis (2006) demonstrated the feasibility of removing nickel as nickel hydroxyl-carbonate using a fluidised bed reactor.

Battistoni and co-workers (1997) investigated the PO_4-P removal from the supernatant of the anaerobic digested sludge in the batch fluidized bed reactor (FBR). The pH was increased by aeration. When the system is aerated, CO_2 is stripped from the system resulting in an increase in pH. Battistoni and co-workers (2002) showed that the efficiency of the FBR on

phosphate removal is highly dependent on contact time (tc) of the solution with the sand particles and also the pH of the system. It was shown that the phosphorus removal in the FBR fits the following model at the pH range between 8.1 and 9.1.

$$removal[\%] = 100 \times (pH - 7.325)\frac{tc}{((pH - 7.325) + 0.371) \times (tc + 0.0196)} \quad \text{Equation 6}$$

$$Conversion[\%] = 100\frac{pH - 7.21}{(pH - 7.21) + 0.38} \quad \text{Equation 7}$$

These models show that a contact time higher than 0.4hr and a pH higher than 8 are required in order to have fines less than 5%. However, it is worth noting that phosphorus was mainly removed as $Ca_5(PO_4)_3OH$ (HAP) from the waste water when this model was derived. Seckler and co-workers (1996) showed that calcium phosphate removal in the fluidized bed reactor is mainly via the aggregation of fines onto the sand particles. It was shown that large amount of fines are formed at the bottom of the reactor and it decreases as the solution move up the along the FBR. Attrition of phosphate particles is significant at the inlet nozzle because high energy dissipation at the inlet points (Seckler et al., 1996)

Costodes and Lewis (2006) showed that high local supersaturation in the precipitation of nickel hydroxyl-carbonate in the inlet nozzle can be reduced by increasing number of feed points into the reactor, thereby distributing the supersaturation along the length of the column. However, the Ca:Mg molar ratio in municipality wastewater system will be higher at the bottom of the reactor if the number of the magnesium dosage feed points along the reactor is increased. Thus, increasing number of feed points is not the best of option for controlling local supersaturation in the wastewater stream since precipitation of calcium phosphate will be favoured at high Ca:P molar ratios. Other alternatives of controlling supersaturation in the fluidized bed reactor are increasing the recycle flow rate and varying the initial reactant concentration.

4. Materials and methods

4.1 Solutions

The chemical analysis of the wastewater was carried out using Atomic Absorption Spectroscopy (AAS) for the cations, a Merck spectroquant ® NOVA 60 for the NH4+ determination and the vanadomolybdophosphoric acid colorimetric method used for the analysis of phosphate (Apha, 1998) (see Appendix A).

Dewatering liquors were collected from municipal sludge from a Tswane wastewater treatment plant. The sludge being dewatered is a combination of an anaerobically digested primary sludge and an undigested waste activated sludge. Nitrogen and Phosphate are released during the anaerobic digestion treatment process. As a result, the concentrations of the wastewater stream treated herein depend mainly on the operational conditions of the anaerobic digestion process. As a result, the wastewater stream may have high elemental variances which have significant impact on the precipitation process. As a result, the samples were collected at two different periods to investigate the feasibility at removing phosphate under different initial wastewater conditions.

Waste water samples with the compositions shown in Table 1 were used in this study.

Table 1: Concentrations of Tshwane Municipality dewatering liquors

Element	Sample C1 Concentration [mg/L]	Sample C2 Concentration [mg/L]
Mg^{2+}	73.4 ± 2.2	27.1 ± 0.5
Ca^{2+}	19.1 ± 0.4	41.7 ± 0.3
K^{+}	88.8 ± 1.8	31.3 ± 0.5
Na^{+}	55.8 ± 1.0	35.1 ± 0.5
Al^{3+}	0.2 ± 0.1	0.5 ± 0.1
PO4-P	145.0 ± 4.3	93.0 ± 2.8
NH4-N	65.2 ± 10.0	57.0 ± 3.2
SO_4^{2-}	23.0	0
HCO_3^{-}	623 ± 24	396
Ca/P molar ratio	0.1	0.35
N/P molar ratio	0.99	1.35

4.2 Aqueous chemistry modelling

Thermodynamic modelling of the aqueous chemistry was carried out using OLI Systems Inc. Stream Analyser Version 2.0.57. The thermodynamic model predicts the behaviour of mixed solvent electrolyte solutions ranging from dilute solutions to the solids saturation. The total excess Gibbs energy of the system takes into account the excess Gibbs energy due to long range electrostatic interactions, short range intermolecular interactions and ion-ion-molecule interactions. The Pitzer-Debye-Huckel expression is used to calculate the long range electrostatic interactions, the UNIQUAC model for the short range intermolecular interactions and second viral equation for ion-ion interactions and ion-molecule interactions (Wang et al., 2008). The standard public OLI databank does not include struvite. As a result an additional struvite database was sourced via OLI Systems Inc. and incorporated into the existing databank.

The effect of varying NH_4^+ and Mg^{2+} in dewatering liquor was carried out by adding NH_4Cl and $MgCl_2.6H_2O$ to the model. The effect of pH on struvite precipitation was investigated by adding NaOH to the model.

4.3 Bench-scale feasibility study

All bench-scale experiments were carried out in a 1L glass reactor. The glass reactor was filled with the wastewater and an initial pH was measured. The Mg^{2+}:PO_4^{3-} molar ratio was adjusted by adding $MgCl_2.6H_2O$. The pH was adjusted by adding 1M NaOH. The experiments were conducted at 3 different pH values (i.e. 8, 9 and 10). The concentration of PO_4^{3-} was measured at different time intervals. The final solution was filtered using a 0.2µm filter and the solid particles were subsequently air dried. The solids were then analysed by X-ray diffraction (XRD). A portion of solid particles were digested in 0.01M HCl solution and then analysed for their chemical composition.

Table 2: Details of the experiments carried out to establish the effect of pH on phosphate precipitation

Run	Waste sample	Mg:P	pH	Ca:P	NH4:P
B1	C1	1:1	8	0.1:1	0.99:1
B2	C1	1:1	9	0.1:1	0.99:1
B3	C1	1:1	10	0.1:1	0.99:1
B4	C2	1:1	9	0.35:1	1.35:1
B5	C2	1:1	10	0.35:1	1.35:1

Table 3: Details of the experiments carried out to establish the effect of Mg:P molar ratio on phosphate precipitation

Run	Waste sample	Mg:P	pH	Ca:P	NH_4:P
B6	C1	1:1	9	0.1:1	0.99:1
B7	C1	1.2:1	9	0.1:1	0.99:1
B8	C1	1.4:1	9	0.1:1	0.99:1
B9	C1	1.6:1	9	0.1:1	0.99:1
B10	C1	1:1	10	0.1:1	0.99:1
B11	C1	1.2:1	10	0.1:1	0.99:1
B12	C1	1.4:1	10	0.1:1	0.99:1

Table 4: Details of the experiments carried out to establish the effect of Ca:P molar ratio on phosphate precipitation

Run	Waste sample	Mg:P	pH	Ca:P	NH4:P
B13	C2	1:1	9	0.35:1	1.35:1
B14	C2	1:1	9	0.6:1	1.35:1
B15	C2	1:1	9	0.85:1	1.35:1

Table 5: Details of the experiments carried out to establish the effect of NH_4^+:P molar ratio on phosphate precipitation

Run	Waste sample	Mg:P	pH	Ca:P	NH4:P
B16	C2	1:1	9	0.35:1	1.35:1
B17	C2	1:1	9	0.35:1	2:1
B18	C2	1:1	9	0.35:1	3:1
B19	C2	1:1	9	0.35:1	4:1

4.4 Pilot scale experiments

Continuous flow experiments were conducted on a larger scale to investigate the feasibility of removing phosphate from the liquor in a pilot scale fluidised bed reactor. The effect of supersaturation on fines formation was investigated by varying Mg^{2+} concentration and by increasing the recycle ratio. A synthetic waste water stream was used in this study. The synthetic waste water stream was prepared by using the following analytical grade Meck chemicals: NH_4Cl, KH_2PO_4, $CaCl_2.2H_2O$, $NaHCO_3$, $Al(OH)_3$ and $MgCl_2.6H_2O$. These chemicals were mixed such that the final concentrations were similar to the concentrations of sample C2 (see Table 1).

4.4.1 Reactor description and sampling

The fluidized bed reactor consisted of a borosilicate glass column, 2.5m high, with an internal diameter of 0.05m. Before each run, the reactor was filled with quartz particles of

between 250 and 500μm diameter. The wastewater and the $MgCl_2.6H_2O$ solution were stored separately in a 200L tank and fed to the reactor through reagent inlet points located at the bottom of the reactor. The pH was measured from a bypass stream at the bottom of the reactor. The pH was controlled by adding NaOH. Figure 8 shows the schematic representation of the experimental setup.

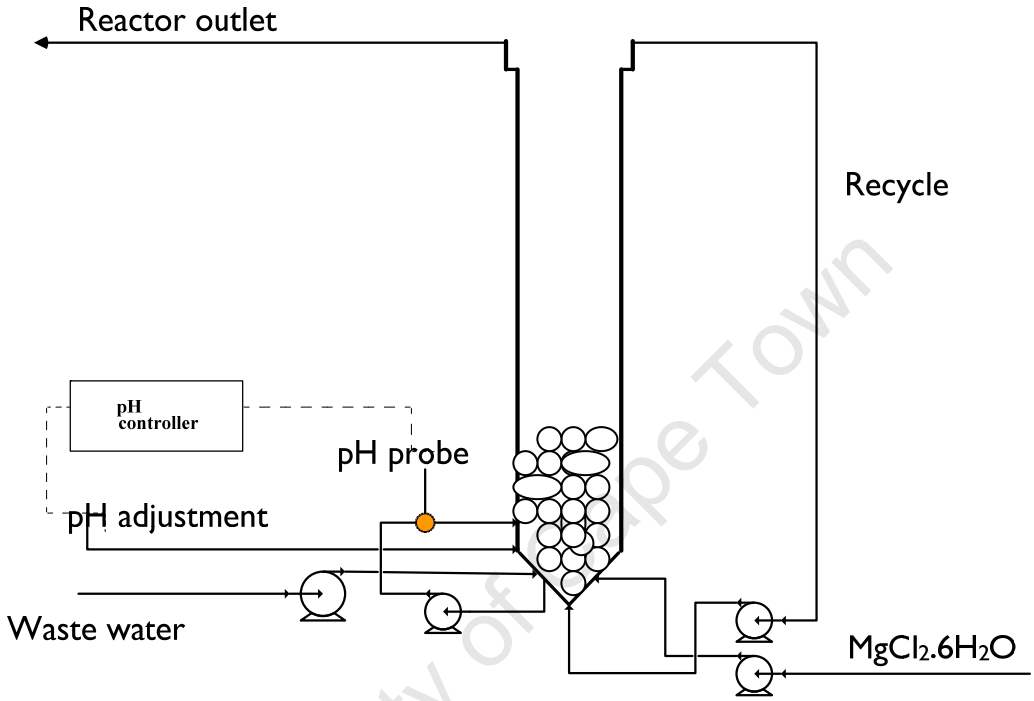

Figure 8: Schematic representation of the experimental setup

Samples were collected at different points along the height of the reactor. Each of the collected samples was divided into two portions. The first portion was filtered though a 0.2μm filter to remove all the suspended solids from the sample. The other portion was digested using a strong sulphuric acid to dissolve the suspended solids. The spent sand was removed from the reactor through an opening at the bottom of the column at the end of each experiment. The method explained in section 4.1 was used to analyse the solid particles and to measure concentrations. The percentage of PO_4-P conversion and removal was calculated using Equation 8 and Equation 9 respectively.

$$\text{Conversion [\%]} = \frac{Mass_{in} - Mass_{dissolved,out}}{Mass_{in}} \quad \text{Equation 8}$$

$$\text{Removal [\%]} = \frac{Mass_{in} - Mass_{total,out}}{Mass_{in}} \quad \text{Equation 9}$$

Where Mass in = C_{in} [mg/L]× inlet flow rate [L/hr]

$Mass_{dissolved, out=}$ = $C_{filtered}$ [mg/L] × outlet flow rate [L/hr]

$Mass_{total\ out}$ = $C_{unfiltered}$[mg/L] × outlet flow rate [L/hr]

C = concentration [mg/L]

Table 6: Inlet flow rates into the FBR

Stream	**Flow rate[L/hr]**
Waste water flow rate	30.25
$MgCl_2.6H_2O$ flow rate	4.93

The recycle ratio was defined as follows:

$$RR = \frac{recycle\_flowrate}{feed\_Flowrate} \quad \text{Equation 10}$$

Table 6 shows the flowrates of the wastewater and the $MgCl_2.6H_2O$ stream used. The inlet flowrates were kept constant in all the experiments conducted in this study. The recycle flowrates were varied from 19.6L/hr (i.e. RR=0.56) to 24.2L/hr (RR= 0.69) in order to investigate the effect of controlling supersaturation by diluting the inlet stream concentration. The Mg: P molar ratio into the system was varied by changing the Mg^{2+} concentration.

5. Results

5.1 Aqueous chemistry modelling of phosphate removal

$Ca_5(PO_4)_3OH$ (HAP) was removed from the modelling database due to the fact that the kinetics of precipitation of this compound are extremely slow. $CaCO_3$ was also removed because previous studies showed that precipitation of $CaCO_3$ is inhibited in the presence of Mg^{2+}, PO_4^{3-} and dissolved organics (Çelen et al., 2007). Sample C1 concentrations were used for the thermodynamic modelling.

Table 7 shows the resulting charge imbalance based on OLI's reconciliation of the stream based on the chemical analysis.

Table 7: Dewatering liquor charge balance (pH 8.6)

	Charge [eq/L]
Cation Charge:	0.008703 eq/L
Anion Charge:	-0.015802 eq/L
Imbalance:	-0.007100 eq/L

Table 7 shows that the chemical analysis has a cation deficiency, which was resolved by adjusting the K^+ ion concentration. The effect of the K^+ ion on struvite precipitation is less significant when compared to the effect of the other ions which either enhance struvite precipitation or the formation of impurities (van Rensburg et al., 2003). An extra 277mg/L of K^+ ions were added to balance the total charge.

5.1.1 The effect of varying waste water conditions using OLI simulation

Figure 9 shows the dominant solids that are formed when the pH is varied without increasing the concentration of Mg^{2+} and NH_4^+ of sample C1. The results show that less than 10% of phosphate is removed as struvite at pH 9 when pH is the only parameter adjusted in the system. Phosphate is mainly removed as $Ca_3(PO_4)_2$ at a pH above 7 and also by $Mg_3(PO_4)_2.8H_2O$ precipitation at pH levels between 9 and 10. Figure 10 shows that the maximum phosphate conversion through $Ca_3(PO_4)_2$ and $Mg_3(PO_4)_2.8H_2O$ precipitation was approximately 13% and 40% respectively. Therefore, it can be concluded that it is not effective to adjust the pH only. The stream (i.e. sample C1) has Mg:P molar ratio of 0.7 but a

ratio of 1.5 is required to completely remove PO_4^{3-} via $Mg_3(PO_4)_2.8H_2O$ precipitation. Therefore, it is necessary to increase Mg^{2+} concentration in the stream.

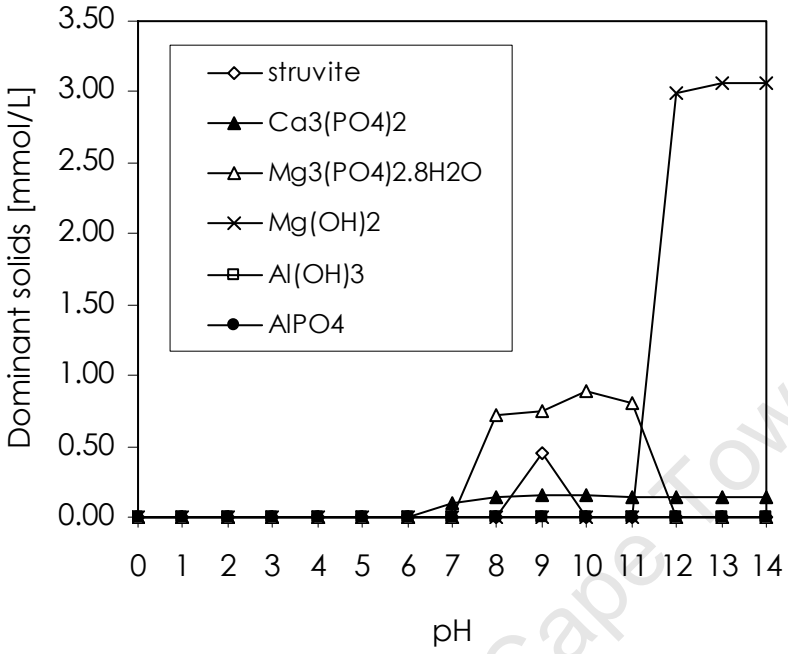

Figure 9 *:* The effect of adjusting the pH of sample C1 without adding NH_4Cl and $MgCl_2.6H_2O$ into the system.

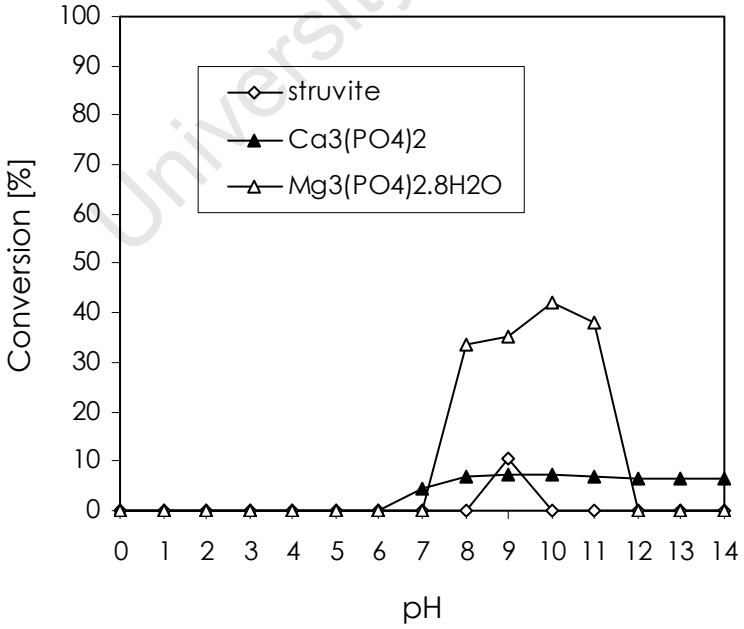

Figure 10: Phosphate conversion at different pH levels when sample C1 concentrations are kept constant.

Figure 11 shows the effect of pH on phosphate removal when the Mg:P molar ratio is increased to 1:1. Approximately 60% and 10% of the phosphates are removed as $Mg_3(PO_4)_2.8H_2O$ and $Ca_3(PO_4)_2$ respectively. It is apparent in Figure 11 that phosphate removal through $Mg_3(PO_4)_2.8H_2O$ precipitation starts at pH above 7 and increases with an increase in pH. However, it reaches a maximum at pH 10 and then reduces to zero. An increase in pH increases the availability of PO_4^{3-} ions required for the $Mg_3(PO_4)_2.8H_2O$ precipitation. However, free Mg^{2+} availability decreases at high pH levels because $Mg(OH)_2$ precipitation is favoured as shown in Figure 12.

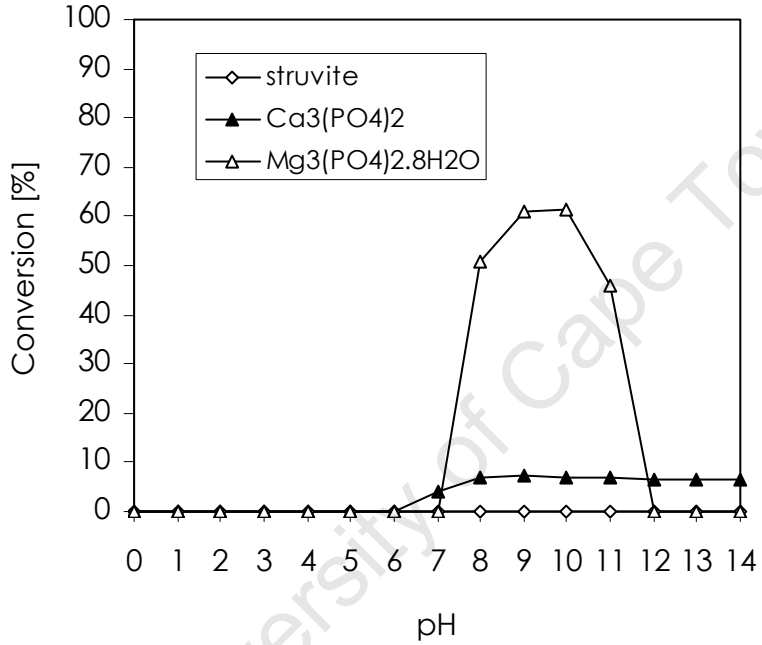

Figure 11: Phosphate conversion at different pH levels when sample C1 Mg:P molar ratio is 1:1

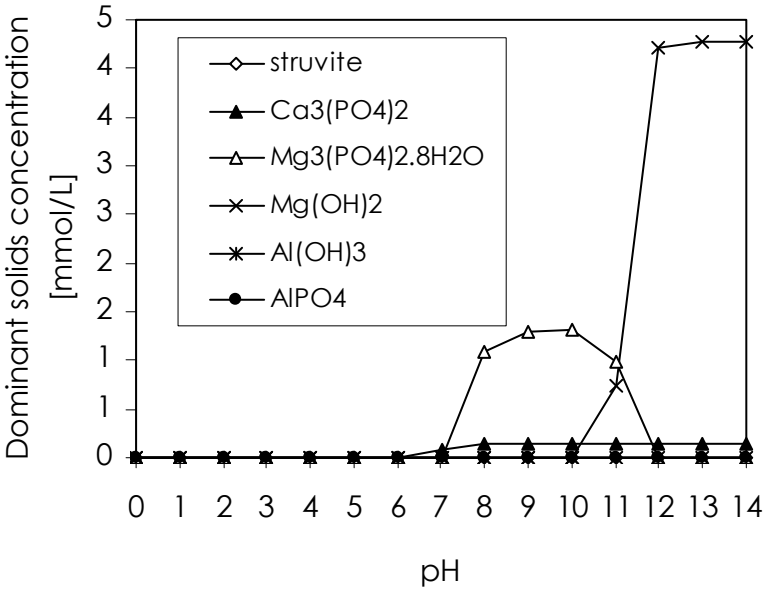

Figure 12: The pH effect when sample C1 Mg:P molar ratio is adjusted to 1:1 by adding $MgCl_2.6H_2O$ into the system

It is worth noting that the thermodynamic model shows the precipitation of the most thermodynamically stable compounds but that the kinetic effects are not accounted for by the modelling. However, as the reaction kinetics also play a significant role, it is possible for an intermediate precipitate to be formed. For example, both struvite and $Mg_3(PO4)_2.22H_2O$ precipitation are possible since the supersaturation ratios are greater than 1 at a pH above 7 as shown in Figure 13.

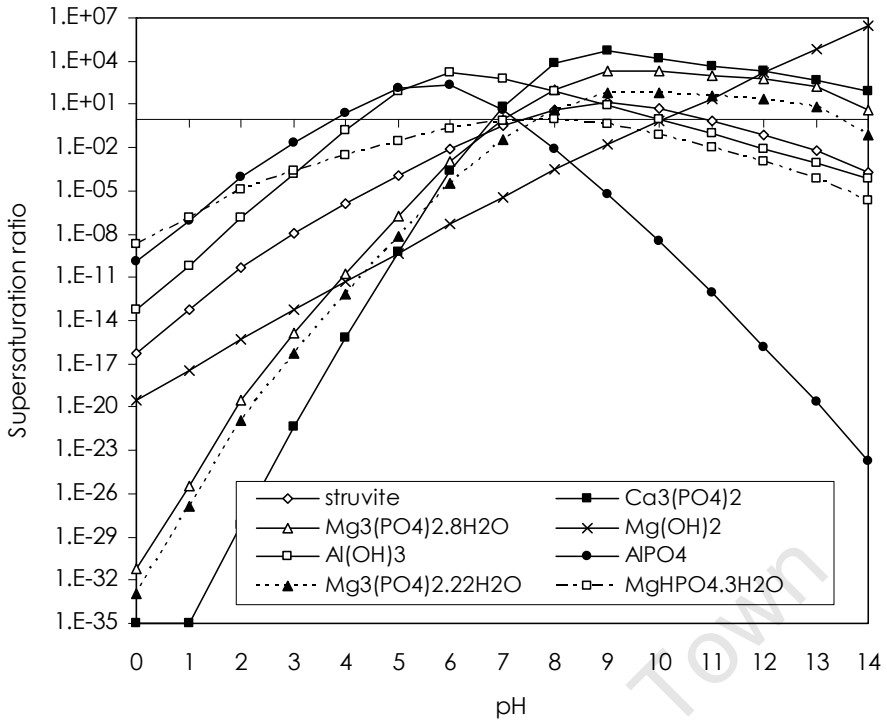

Figure 13: The effect of pH on supersaturation ratio (OLI Systems Inc, 2008)

Figure 14 and Figure 15 show the effect of increasing the Mg:P molar ratio by adding $MgCl_2.6H_2O$ in the wastewater stream. It is evident that an increase in Mg:P molar ratio favours phosphate removal as $Mg_3(PO_4)_2.8H_2O$ and decreases struvite precipitation. However, it does not have a significant effect on the precipitation of $Ca_3(PO_4)_2$. This is due the fact that $Ca_3(PO_4)_2$ supersaturation is very high compared to the magnesium phosphate compounds as shown in Figure 16.

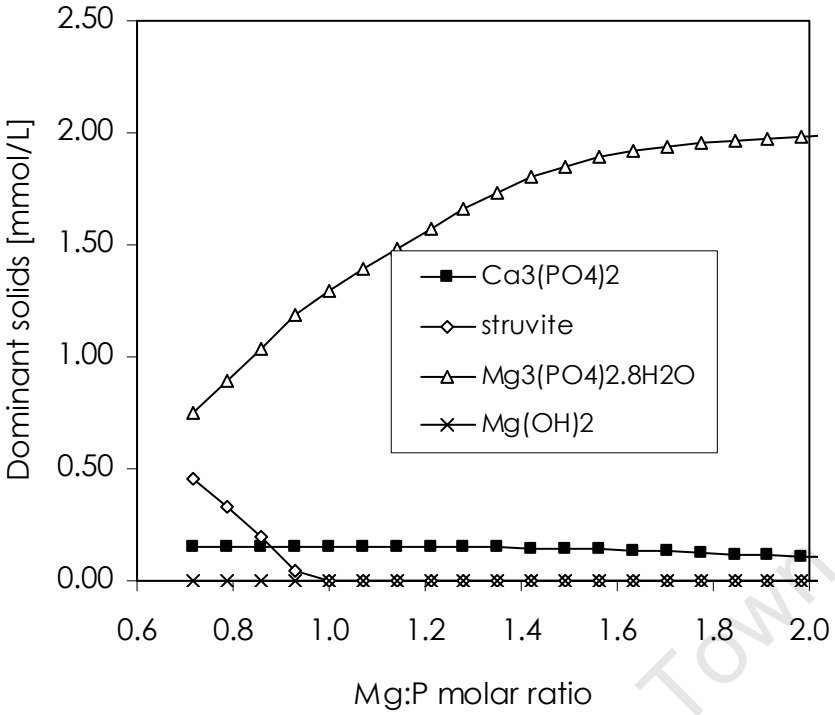

Figure 14: The effect of increasing the Mg^{2+}:P molar ratio of sample C1 by adding $MgCl_2.6H_2O$ under pH 9 conditions.

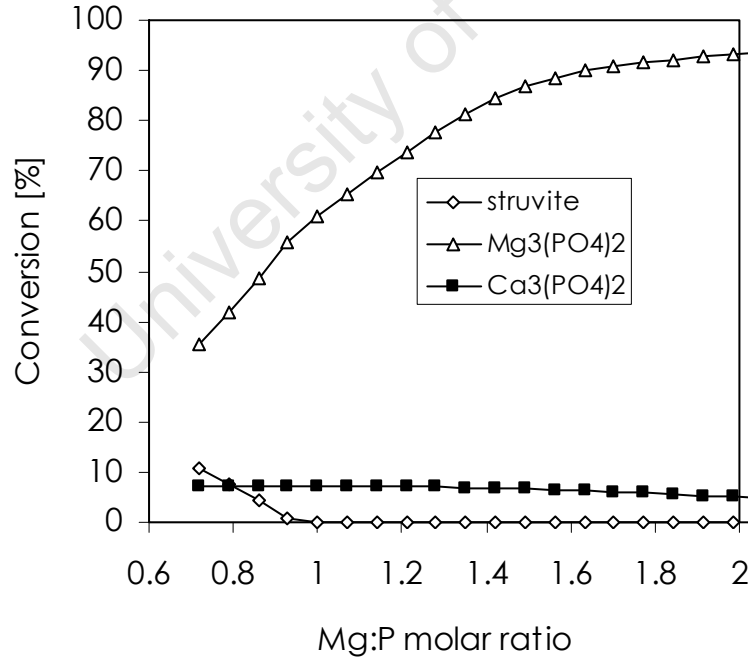

Figure 15: Phosphate conversion at different Mg^{2+}: P molar ratios under pH 9 conditions

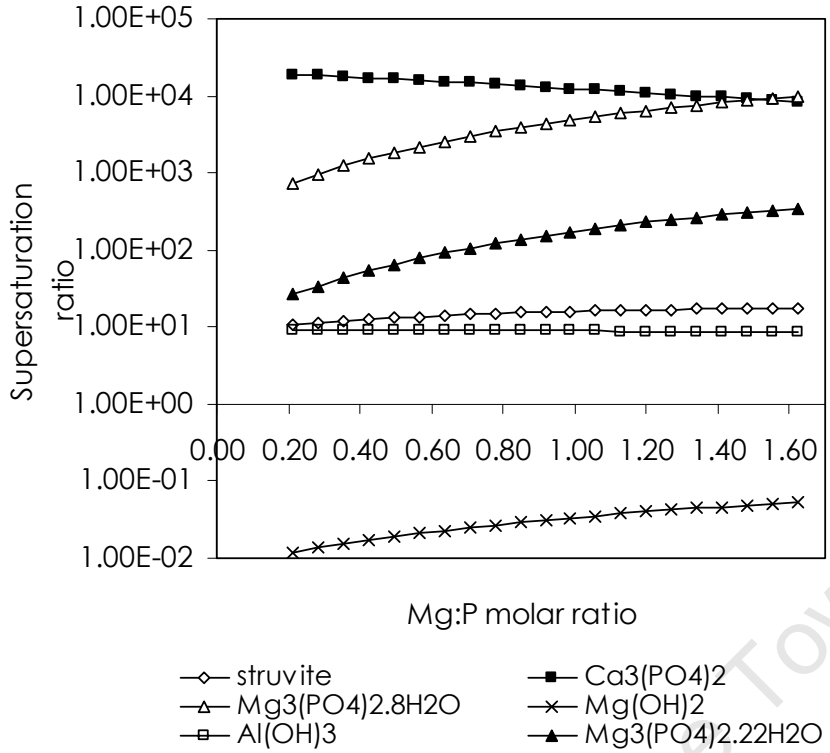

Figure 16: The effect of Mg:P molar ratio on supersaturation under pH 9 conditions

Figure 17 shows the effect of increasing the NH_4^+ ion concentration with the addition of NH_4Cl. The results show that struvite precipitation is induced by increasing the NH_4^+:P molar ratio while formation of $Mg_3(PO4)_2.8H_2O$ decreases at high NH_4^+:P molar ratio. Approximately 80% of phosphates are removed as struvite at a NH_4^+:P molar ratio of 2.5:1. The $Mg_3(PO_4)_2.8H_2O$ precipitation decreases as the NH_4^+:P molar ratio increases whilst there is no significant effect on $Ca_3(PO_4)_2$ precipitation.

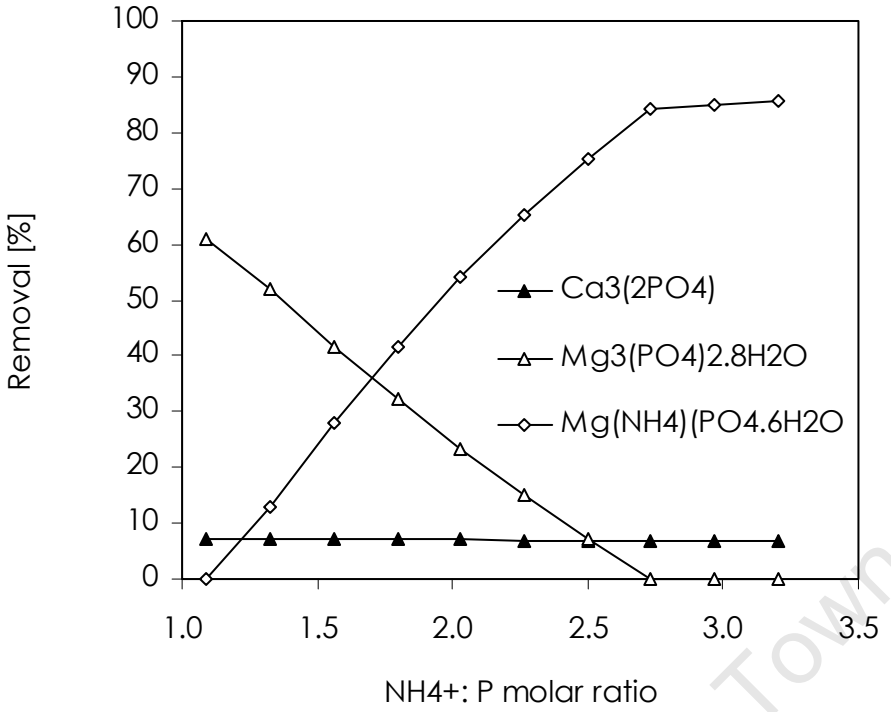

Figure 17: The effect of increasing the NH_4^+:P molar ratio of sample C1 under pH 9 conditions and Mg:P molar ratio of 1:1

5.2 Bench-scale experiments

5.2.1 The effect of pH on phosphate conversion at Mg: P molar ratio of 1:1

Figure 18 and Figure 19 show the concentration of the PO_4-P and the total phosphate at different pH levels respectively. Figure 20 and Figure 21 show the ortho-phosphate (PO_4-P) and total phosphate conversion of sample C1 under different pH conditions. Approximately 92% and 30% PO_4 -P conversion is achieved within 60 minutes at pH 10 and 8 respectively. It is worth noting that the reaction time required for high phosphate conversion is achieved within 60 min at high pH levels. Therefore, an increase in residence time does not play a significant role in increasing the phosphate conversion because the reaction has fast kinetics. This is consistent with previous studies (Ali and Schneider, 2006; Doyle and Parsons, 2002; Seckler et al., 1996; Pastor et al., 2008) which showed that pH had a significant effect on phosphate conversion due to the fact that an increase in pH increases the availability of free PO_4^{3-}P. As a result, the magnesium and calcium conversion increases via magnesium phosphate and calcium phosphate precipitation as shown in Figure 22.

Table 8 shows that K^+ and Al^{3+} concentrations did not change significantly when sample C1 pH level was varied. This is in agreement with the findings by van Rensburg and co-workers (2003) suggesting that K^+ ion in the anaerobic digester liquors does not participate in the precipitation reactions.

After 22 hrs the ortho-phosphate (PO_4-P) and total phosphate removal at pH 10 were approximately 84% and 70%, respectively. It is worth noting that 100% total phosphate removal is not feasible since the poly-phosphate does not participate in the chemical reaction. Polyphosphates are phosphate polymers that are stored within the biomass in the biological nutrient removal process (Doyle et al., 2000). In the anaerobic digestion process, the re-hydrolysis of polyphosphate to PO_4-P ions occurs (Doyle et al., 2000). PO_4-P ions in solution are those required for phosphate precipitation. Thus, improving the efficiency of the anaerobic digestion ensures that the polyphosphates concentration is reduced. However, the primary focus of this project was on the treatment of anaerobic digested effluent stream.

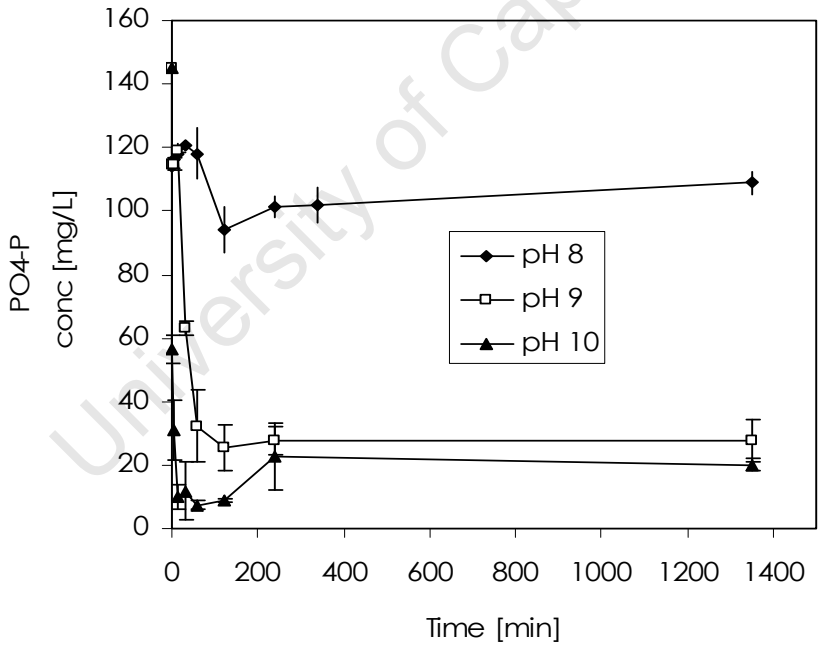

Figure 18: Sample C1 ortho-phosphate (PO_4-P) concentrations with reaction time at different pH values

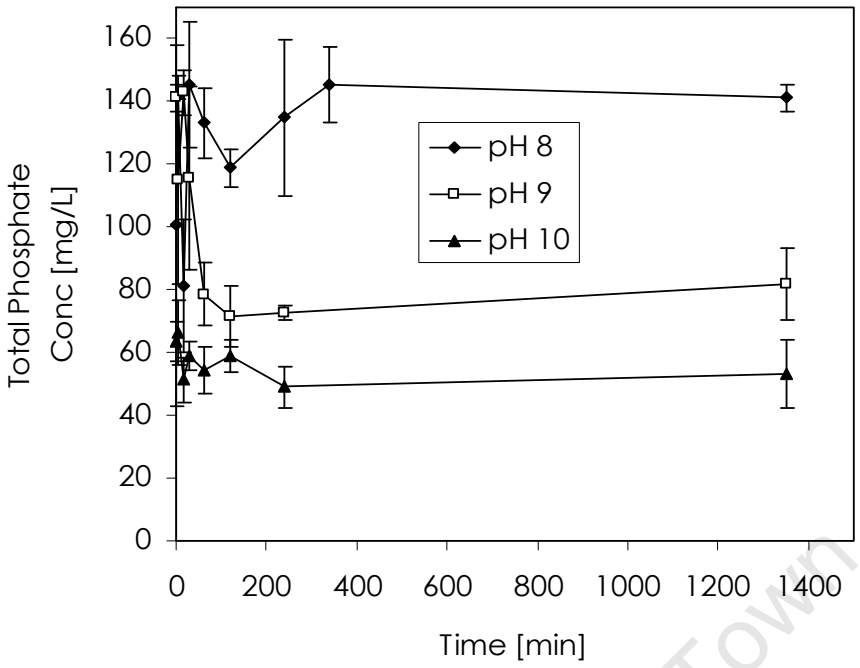

Figure 19: Sample C1 total phosphate (P) concentration with reaction time at different pH values

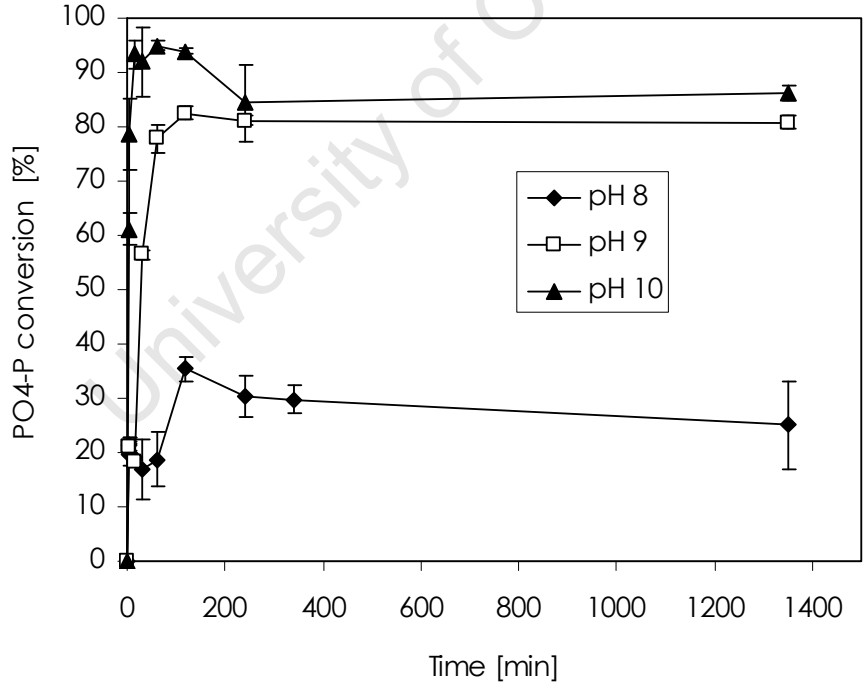

Figure 20: Sample C1 ortho-phosphate (PO_4-P) removal with reaction time at different pH values

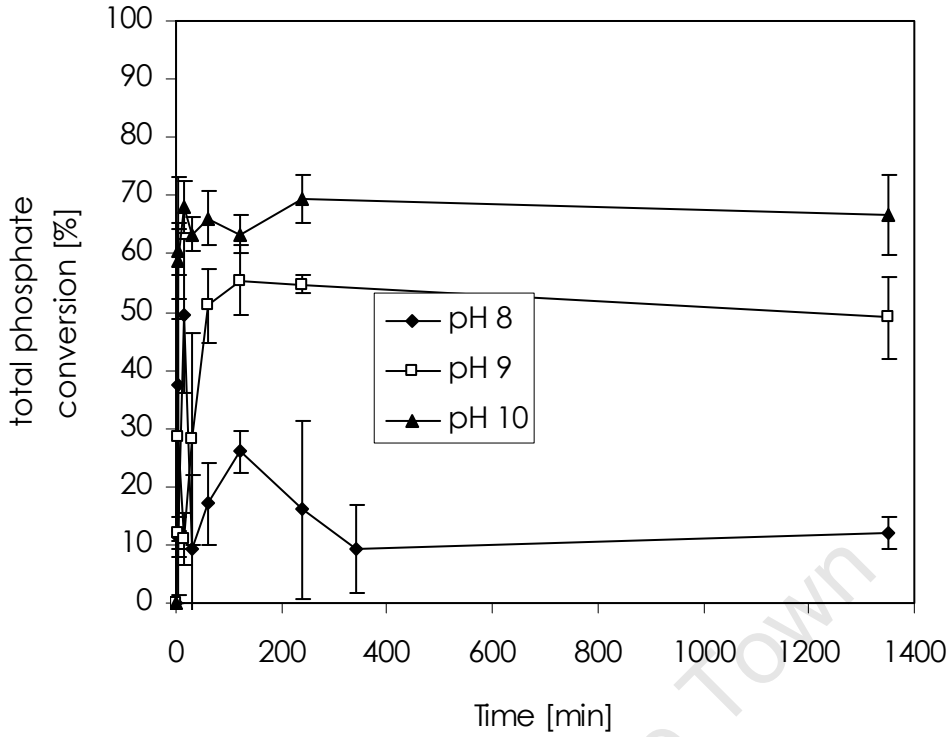

Figure 21: Sample C1 total phosphate (P) conversion with reaction time at different pH values

Table 8: Final concentrations of sample C1 at different pH values

Element [mg/L]	pH 8	pH 9	pH 10
Ca^{2+}	13.9	3.8	2.6
Mg^{2+}	110.1	40.4	20.2
K^{+}	69.5	69.5	71.2
Al^{3+}	0.10	0.1	0.09
$PO_4^{3-}P$	108.8	27.8	20.2

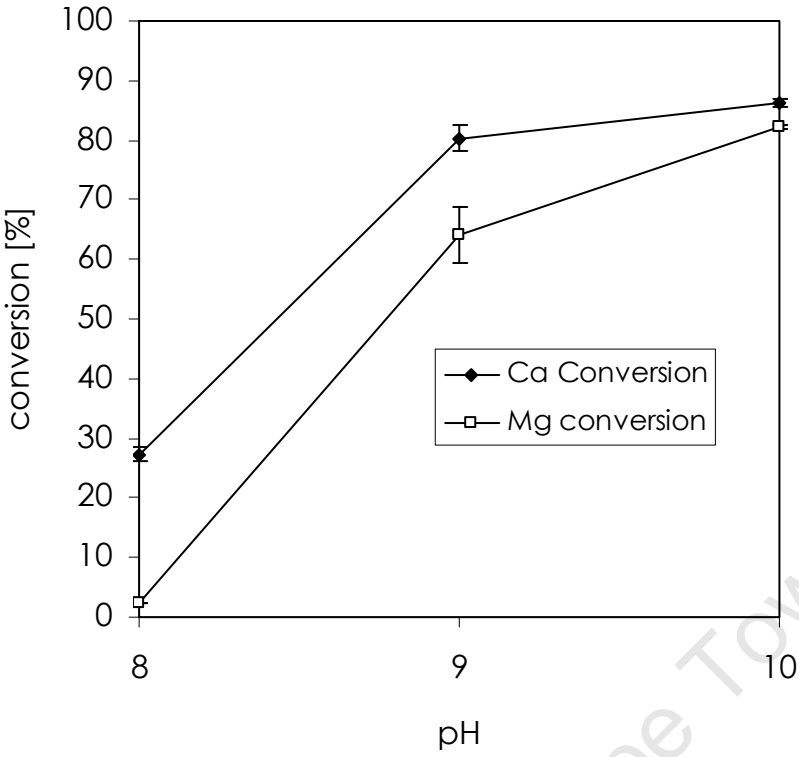

Figure 22: Final Mg^{2+} and Ca^{2+} conversion for sample C1 at different pH values

The Mg:P molar ratio in the final precipitated solids is 1.6 for sample C1 at pH 9 and pH 10. Hence, it can be concluded that phosphorus is precipitating mainly as $Mg_3(PO_4)_2.xH_2O$ because the ratio of Mg:P is 1.5:1. This was verified by XRD which confirmed the solid precipitate to be $Mg_3(PO_4)_2.22H_2O$.

The effect of increasing the pH on phosphate conversion from pH 9 to pH 10 was very small but there was a significant change in the composition of the precipitated solid. The difference of phosphorus conversion at pH 9 and 10 was less than 5%. However, there was a significant difference in the precipitate formed under these conditions. Figure 23 shows that the molar ratio of the NH_4^+:P of precipitated solids changed from 0.26 to 0 when the sample C1 pH was changed from pH 9 to pH 10 conditions.

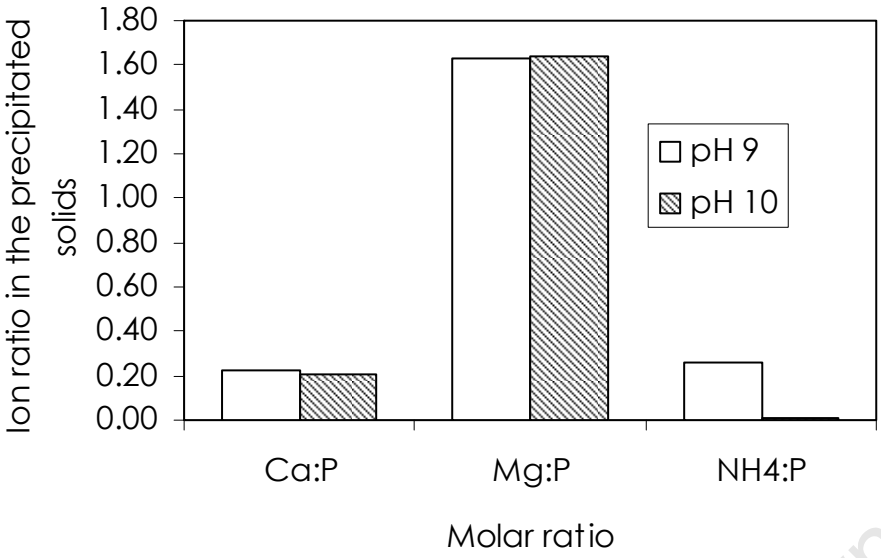

Figure 23: The effect of pH on the ion ratio of the precipitated solids when sample C1 was used

This pH effect on the composition of precipitated solids is significant when the waste stream contains a high NH_4^+:PO_4^{3-} molar ratio. Figure 24 shows that when sample C2 is under pH 9 conditions struvite precipitate is formed while under pH 10 conditions $Mg_3(PO_4)_2.22H_2O$ is the dominant solid. Furthermore, pH affected the morphology as shown by Figure 35 A and B when the pH is changed from pH 9 to pH 10. Thus, high pH values increase the availability of free PO_4^{3-}P but also decrease the amount of free NH_4^+ and free Mg^{2+} required for struvite ($MgNH_4PO_4.6H_2O$) precipitation. Mg^{2+} changes to $MgOH^+$ at higher pH values and NH_4^+ is converted to NH_3 at high pH levels. As a result, the removal of phosphate as struvite is limited at high pH levels. On the other hand, calcium removal increases with an increase with pH. Therefore, it can be concluded that the optimum pH for phosphate and NH_4^+ removal is pH 9. The findings of the investigation of the effect of high NH_4^+:PO_4^{3-}molar ratio is discussed in section 5.2.4 .

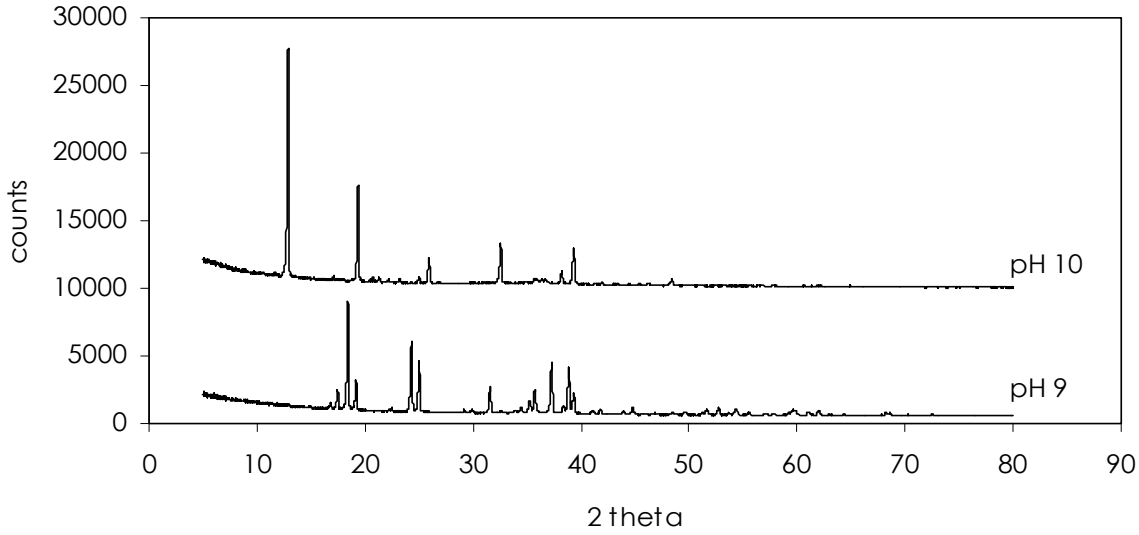

Figure 24: The X-ray diffraction (XRD) of final precipitate formed under different initial pH values of sample C2

5.2.2 The effect of increasing the Mg: P molar ratio on phosphate precipitation

Figure 25 and Figure 26 show the change in PO_4^{3-}-P concentrations at different Mg:P molar ratios for the sample C1 under pH 9 and pH 10 conditions respectively. It is apparent from these figures that an increase in Mg:P molar ratio increases the conversion of phosphorus. However, a significant increase in phosphorus removal is evident when the stream is under pH 9 conditions. For example, the phosphorus removal increases from 80% to 100% when the Mg:P is increased from 1:1 to 1.2:1 as shown in Figure 27. On the other hand, phosphorus removal increases slightly by approximately 8% when Mg: P is increased from 1:1 to 1.2:1 for the system under pH 10 conditions as shown in Figure 28. An increase in Mg:P molar ratio increases the amount of free Mg^{2+} required for phosphorus precipitation. Consequently, high conversions are achieved at high Mg:P molar ratios. However, when the system is under pH 10 conditions $MgOH^+$ formation is also favoured. Consequently, the availability of free Mg^{2+} required for phosphate precipitation is reduced. As a result, the effect of increasing Mg:P on phosphate precipitation is significant at pH 9 conditions. This is consistent with previous studies which showed additional benefit of increasing Mg:P on phosphate conversions at lower pH values (Nelson et al., 2003).

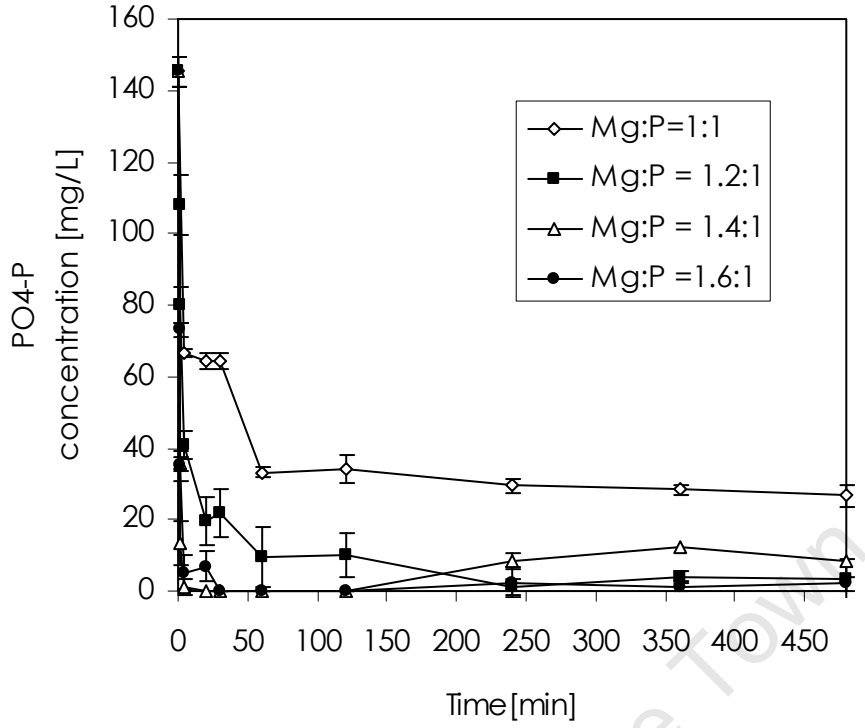

Figure 25: PO_4-P concentration with reaction at different Mg: P molar ratios under pH 9 conditions

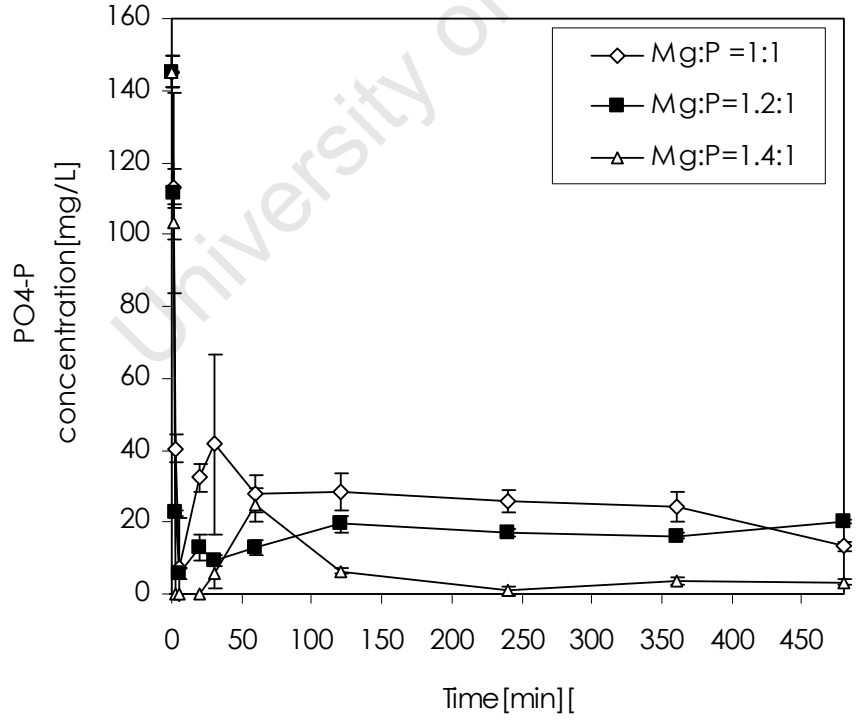

Figure 26: Sample C1 PO_4-P concentrations with reaction at different Mg:P molar ratios under pH 10 conditions

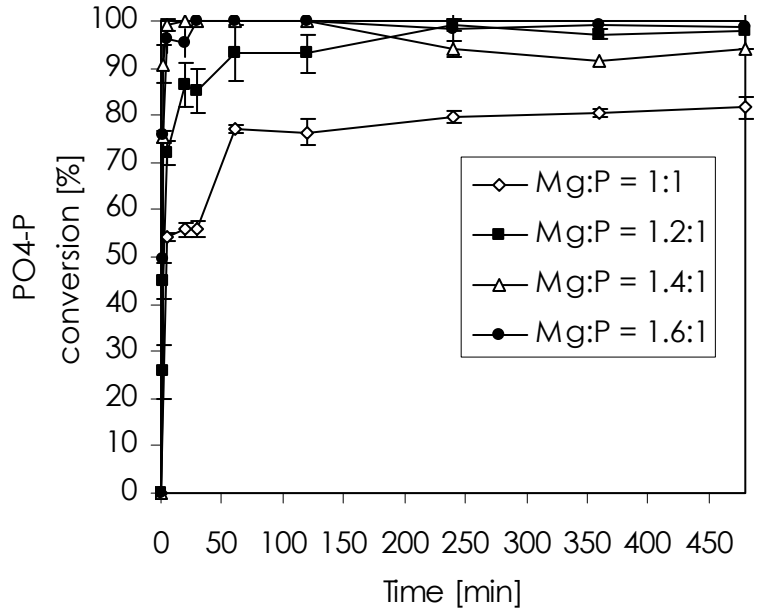

Figure 27: The effect of Mg: P molar ratio on P removal under pH 9 conditions

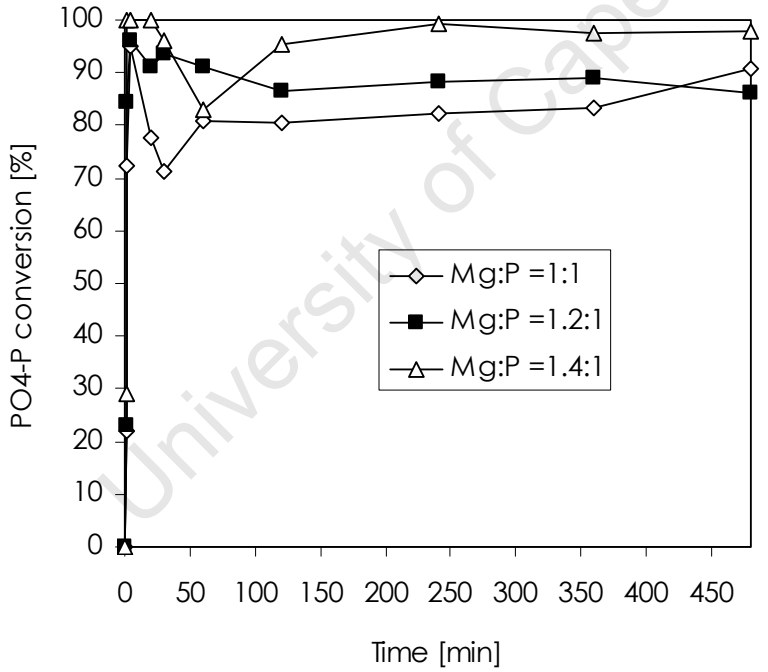

Figure 28: The effect of Mg:P molar ratio on PO_4-P conversion when sample C1 is under pH 10 conditions

Moreover, the conversion of phosphorus as amorphous calcium compounds is also slightly reduced at high Mg:P molar ratios as shown in Figure 29. It can be seen that the calcium conversion is reduced by approximately 10% when Mg:P is increased from 1:1 to 1.4:1 for the system under pH 9 conditions and also under pH 10 conditions. In addition, Figure 32

shows that the calcium content in the precipitated solids decreases when the initial Mg:P molar ratio is increased. The effect of Mg: P on phosphorus removal observed in this study is in agreement with previous studies which showed the advantages of additional Mg^{2+} ions in limiting the precipitation of undesirable amorphous calcium compounds. It is worth noting that the supersaturation ratio of Ca compounds is 10^4 greater than the magnesium compounds supersaturation ratio as shown by the thermodynamic model. As a result, the effect of increasing Mg: P on reducing calcium conversion is very small as shown in the thermodynamic modelling results.

The XRD analysis showed that the precipitated solid under all the conditions was $Mg_3(PO_4)_2.22H_2O$. Calcium compounds were not detected on the XRD analysis. The XRD shows that there are no calcium crystalline compounds on the precipitate formed. However, the background noise on the XRD analysis shows the presence of amorphous compounds. Hence, it can be concluded that calcium precipitated as ACP ($Ca_3(PO_4)_2$). It is also worth noting that previous studies show that $Mg_3(PO_4)_2.8H_2O$ is formed in the system with low NH_4^+ and high PO_4^{3-} -P. However, in this study $Mg_3(PO4)_2.22H_2O$ was formed, which corresponds to the compound formed by Le Corre and co-workers (2007).

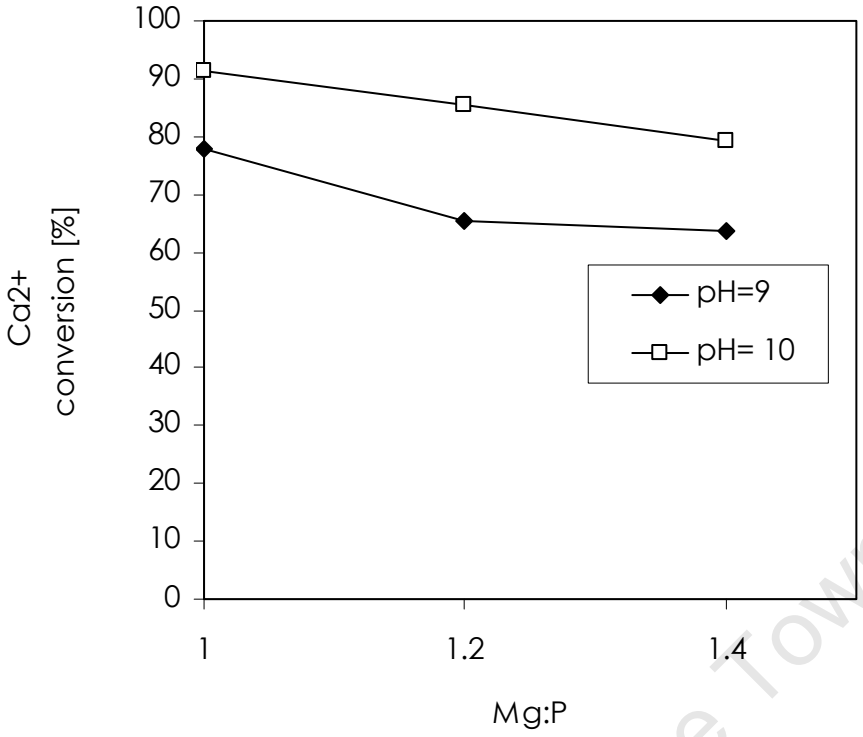

Figure 29: The effect of Mg:P molar ratio on Ca conversion at different pH values for sample C1

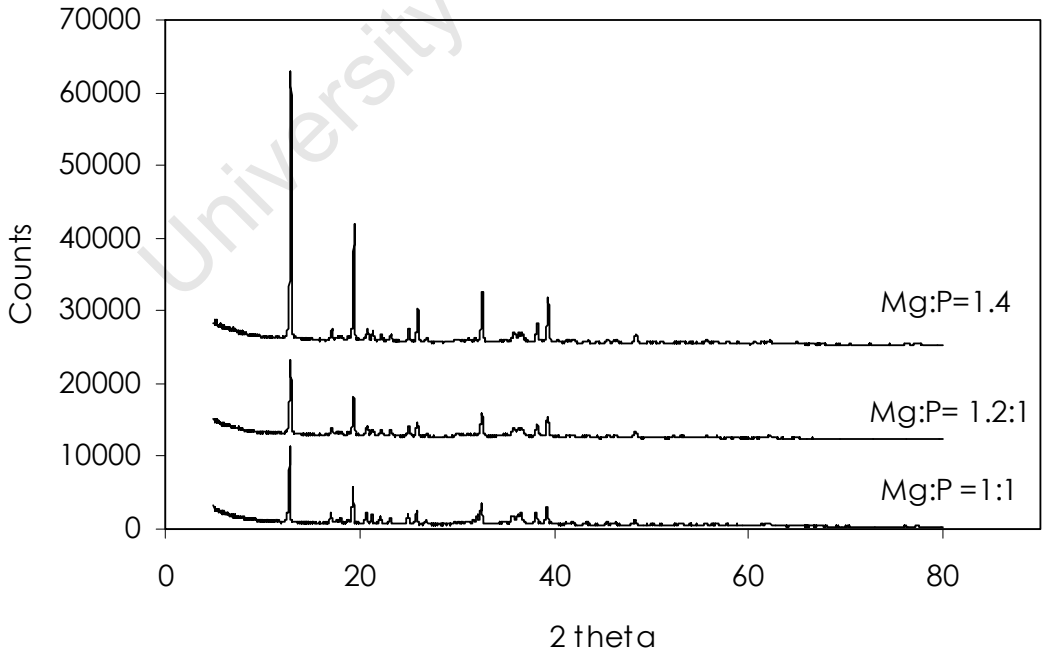

Figure 30: X-ray diffraction of precipitate formed under pH 9 conditions and different Mg:P molar ratios for sample C1

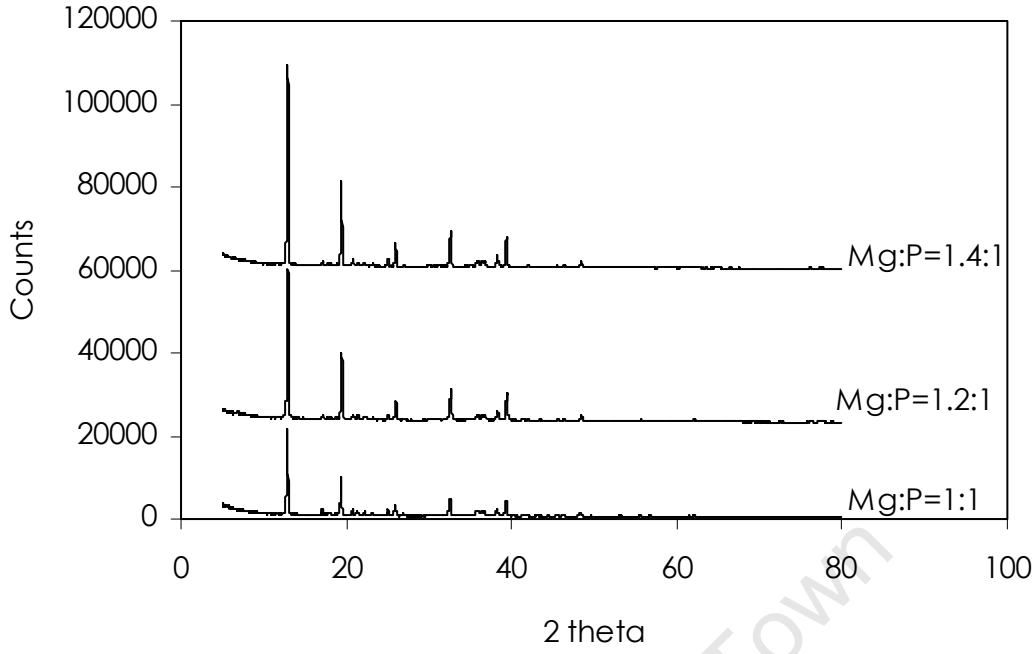

Figure 31: X-ray diffraction of the precipitate formed under pH 10 conditions and different Mg:P molar ratios for sample C1

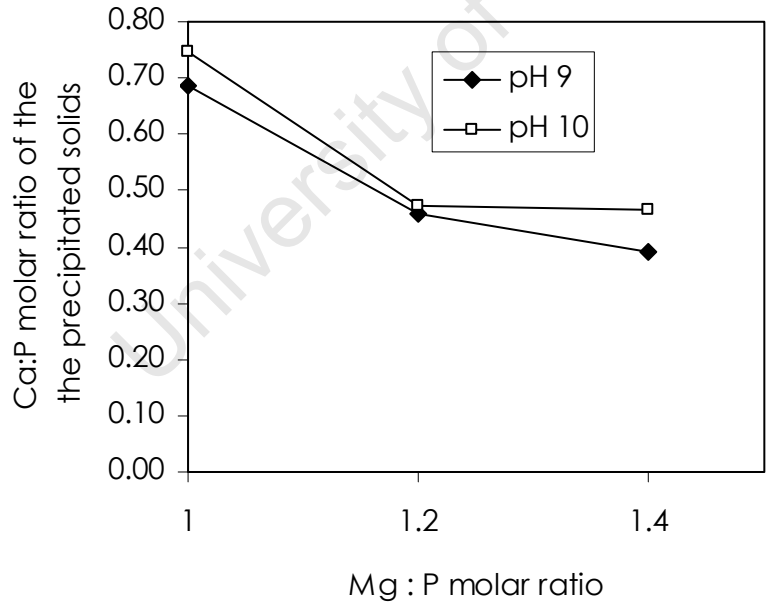

Figure 32: Ca:P molar ratios of the precipitated solids at different initial Mg:P molar ratios for sample C1

5.2.3 The effect of increasing Ca: P molar ratio on phosphate conversion

Figure 33 shows that increasing the Ca:P molar ratio does not have a significant effect on the phosphate removal. However, a high Ca:P molar ratio has a significant effect on the

morphology of the precipitates as shown by SEM pictures in Figure 35 A, C and D. It is apparent in Figure 35 A that at the Ca: P=0.35 the precipitates have an orthorhombic shape (rod shape). This is the expected struvite morphology (Le Corre et al., 2005). The XRD analysis shown in Figure 36 confirms that the precipitates are struvite. The XRD showed that a high background noise when the Ca: P molar ratio is 0.85:1. The calcium concentration in solution decreases with time as shown in Figure 34. Since no other crystalline calcium compounds (e.g. $CaCO_3$) are shown on the XRD it can be concluded that calcium is removed as amorphous compounds (Le Corre et al., 2005). This is in agreement with previous studies by Le Corre and co-workers (2005) and Jaffer and co-workers (2001) which showed that a high calcium concentration in wastewater leads to the formation of amorphous calcium and inhibits struvite precipitation.

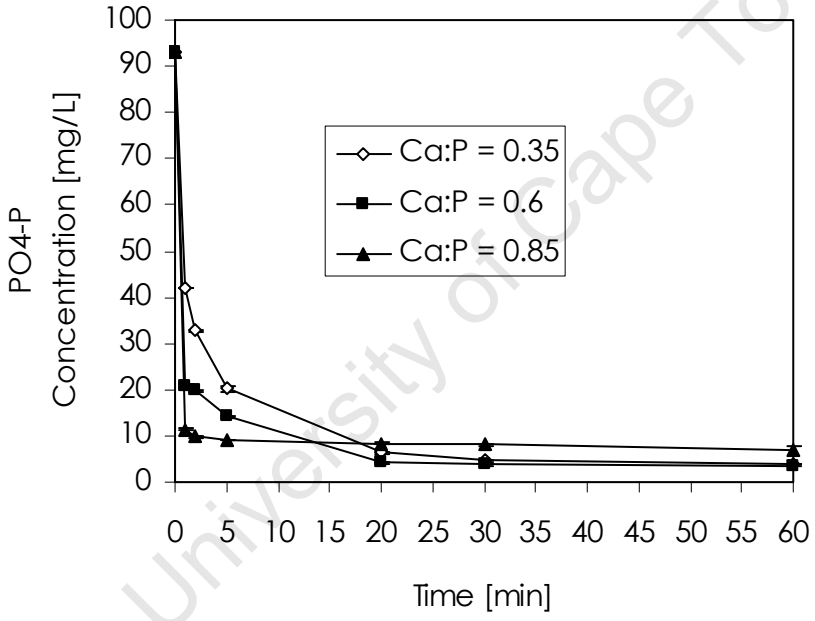

Figure 33: PO_4-P concentration with reaction time at different Ca: P molar ratios when Mg:P molar ratio is 1:1 and pH =9 for sample C2

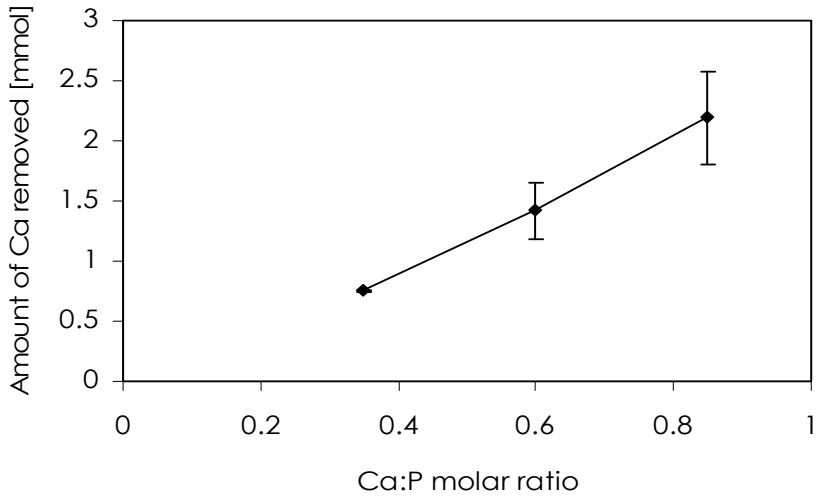

Figure 34: Amount of Ca^{2+} removed at different Ca:P molar ratios when Mg:P molar ratio is 1:1 and pH =9 for sample C2

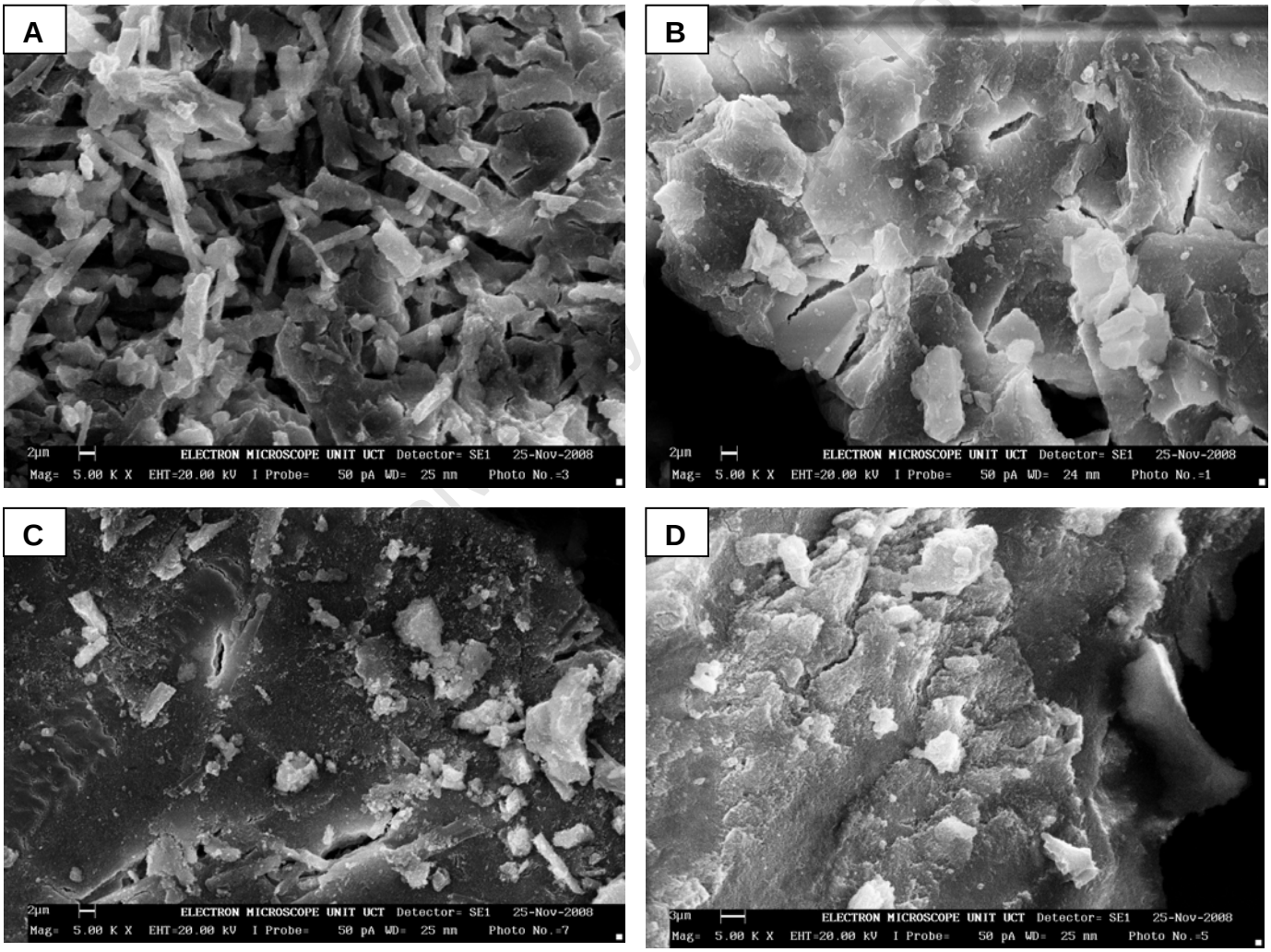

Figure 35: SEM pictures of the precipitates formed under different conditions.
A: Ca:P=0.35 and pH 9, B: pH 10 and Ca:P=0.35, C: pH 9 and Ca:P =0.6, D: pH 9 and Ca:P=0.85

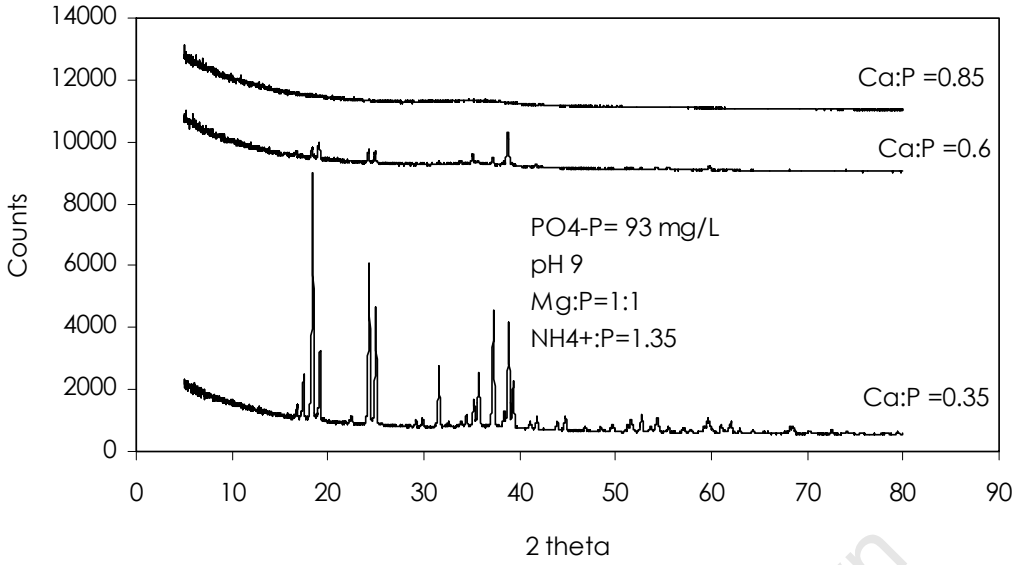

Figure 36: The X-ray diffraction of the precipitates formed at different initial Ca:P molar ratios under pH 9 conditions for sample C2.

5.2.4 The effect of high NH_4^+ concentrations on phosphate precipitation

The effect of a high NH_4^+:P molar ratio is investigated by comparing sample C1 and sample C2 which have different initial N:P molar ratios of 0.99 and 1.35 respectively. Figure 37 shows that the phosphate conversion for sample C2 is higher than the phosphate conversion of sample C1 under pH 9 conditions. Furthermore, the XRD analysis shows that the dominant solids formed were $Mg_3(PO4)_2.22H_2O$ for sample C1 and struvite for sample C2. It is clear that high NH_4^+:P molar ratio favours formation of struvite particles. This is in agreement with previous studies by Ryu et al., (2007); Stratful et al., (2001) & Warmadewanthi and Liu, (2008) which showed that transportation of NH_4^+ to the crystal surface was more favourable at high NH_4^+:P molar ratios.

The concentration of NH_4^+ in sample C2 was increased to investigate the effect of further increasing NH_4^+:P molar ratio by dosing with NH_4Cl. Figure 37 shows that phosphate removal increases from 80% to approximately 90% when the NH_4^+:P molar ratio is increased from 1.35:1 to 2:1. Thereafter, a further increase in NH_4^+:P molar ratio resulted in a relatively insignificant increase of phosphate removal. Importantly, the calcium conversion decreases significantly when the NH_4^+:P molar ratio is increased. For example, the calcium conversion decreased from 80% to 60% when the NH_4^+:P molar ratio is increased from 1.35 to 4. On the other hand, the magnesium conversion increased from 40% to 60%. This counter effect between calcium and magnesium is due to precipitation of struvite induced at high NH_4^+:P

molar ratios. Thus, the formation of amorphous calcium phosphates precipitation is limited while the struvite purity increases at high NH_4^+:P molar ratios.

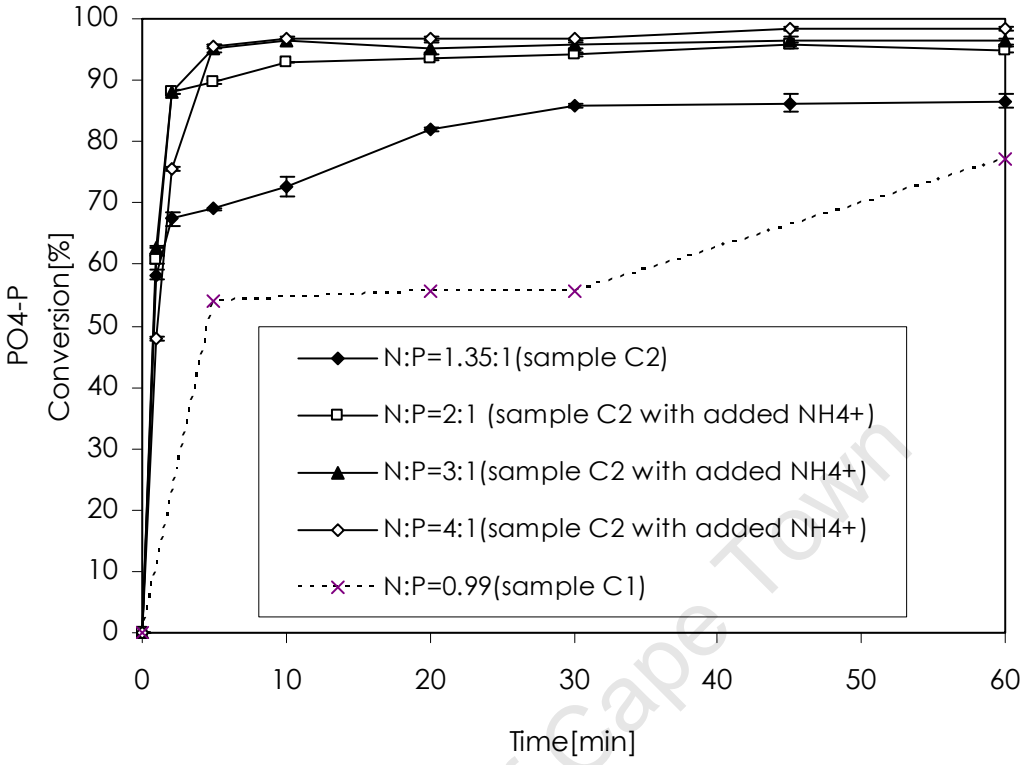

Figure 37: Phosphate removal at different NH_4^+:P when Mg:P Molar ratio is 1:1 at pH 9

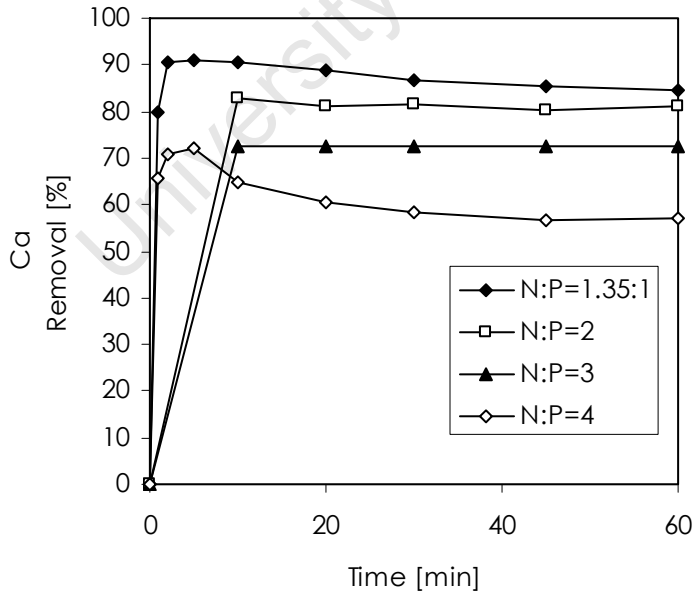

Figure 38: Calcium removal at different NH_4^+:P molar ratio when Mg:P=1:1 under pH 9 conditions for sample C2

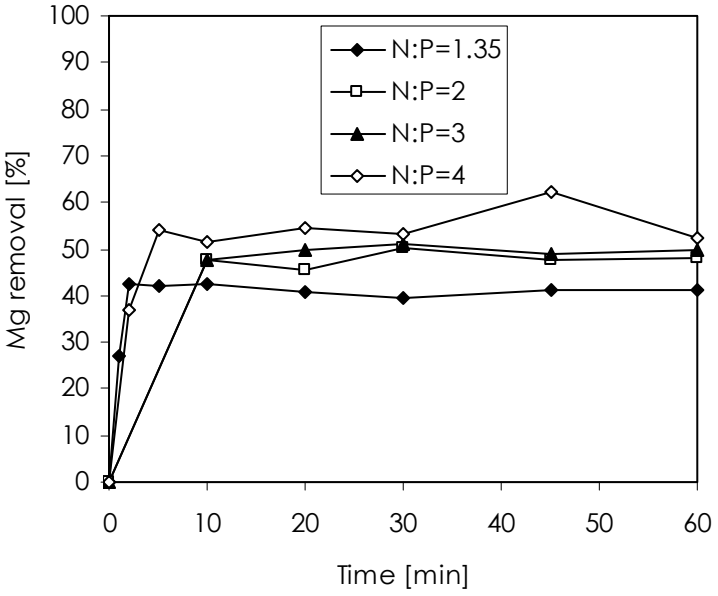

Figure 39: Magnesium removal at different NH_4^+:P Molar ratio when Mg:P=1:1 under pH 9 conditions for sample C2

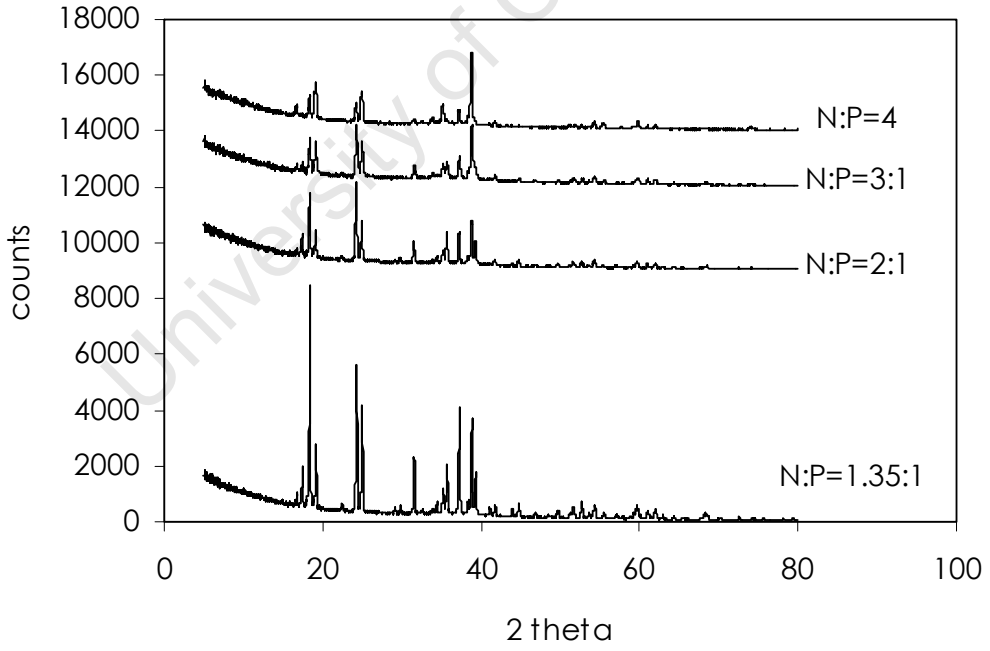

Figure 40: The X-ray diffraction patterns of the precipitate formed at different initial N:P molar ratios under pH 9 conditions for sample C2.

5.3 Pilot scale results

Figure 41 shows that the PO_4-P concentration 30cm above the feed point was the same as the PO_4-P concentration leaving the reactor (i.e. 250cm above the feed point). Thus, the overall conversion was achieved immediately after mixing the waste water stream with the Mg^{2+} stream at the bottom of the reactor. This is due to the very rapid kinetics of PO_4-P as shown in the bench scale experiments. Thus, it can be concluded that the residence time of the solution in the FBR is not a significant factor affecting the conversion. It is apparent in Figure 42 that the total PO_4-P concentration was also constant. Thus, secondary particle formation mechanisms such as attrition and aggregation did not play a significant role in phosphate removal.

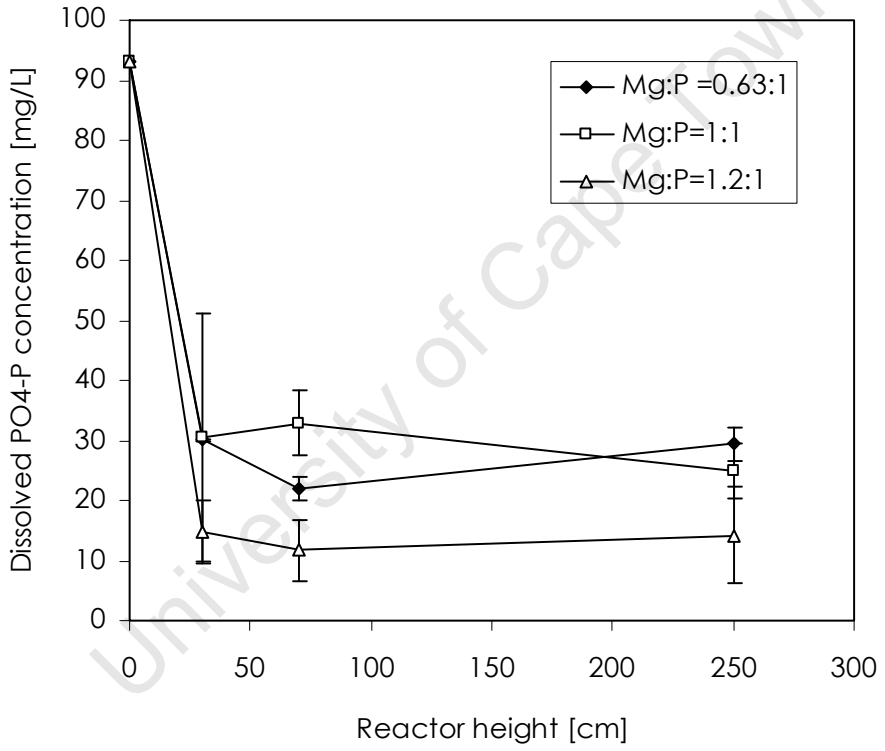

Figure 41: Dissolved PO_4-P concentration under pH 9 conditions at different sampling points along the FBR with a recycle ratio of 0.69

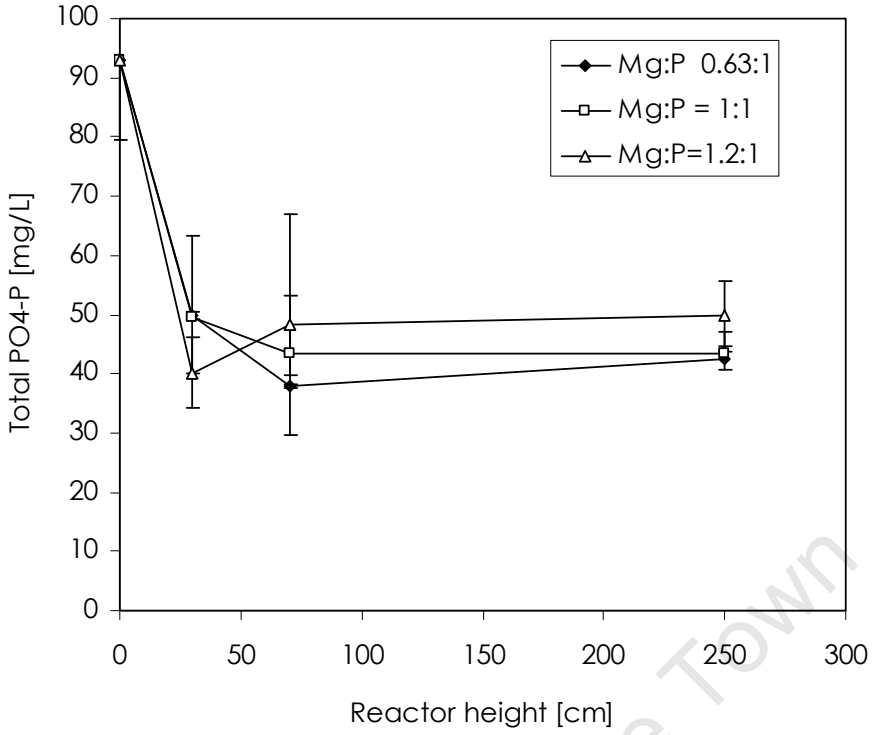

Figure 42: Total PO_4-P concentration under pH 9 condition at different sampling points along the FBR with a recycle ratio of 0.69

It is apparent in Figure 43 that an increase in the initial Mg:P molar ratio increases the overall conversion of PO_4-P. The PO_4-P conversion increased from 68% to approximately 83% when the Mg:P molar ratio was increased from 1:1 to 1.2:1. An increase in Mg:P molar ratio increases the availability of free Mg^{2+} ions required for the precipitation of magnesium phosphate compounds. Consequently, high conversions are achieved at high Mg:P molar ratios. This is consistent with the bench scale experiments and thermodynamic modelling results which showed high PO_4-P conversions at high Mg:P molar ratios. However, the high Mg:P molar ratios increase the level of supersaturation of the magnesium phosphate compounds. High supersaturation levels lead to rapid homogenous nucleation, which results in the formation of numerous fine particles. As a result, the removal of PO_4-P decreased when the initial Mg:P molar ratio is increased, as shown in Figure 43. The removal decreased slightly from 45% to 38% when the Mg:P molar ratio was increased from 1:1 to 1.2:1. Figure 44 shows the particle size distribution (PSD) of the particles leaving the fluidised bed reactor. The average particle size range of the particles was approximately 10 µm.

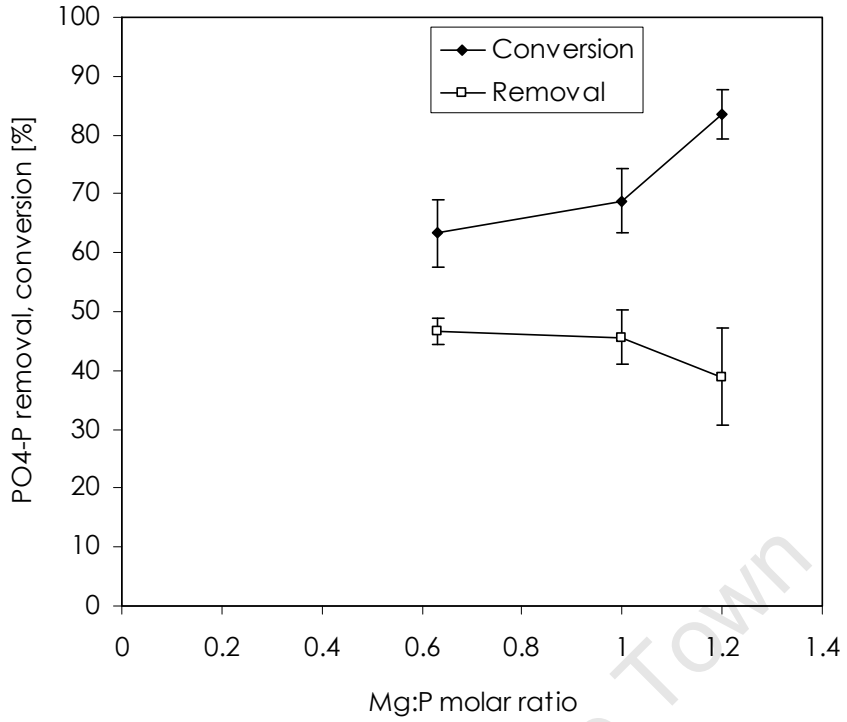

Figure 43: The effect of increasing Mg:P molar ratio on PO_4-P removal and conversion under pH 9 conditions with a recycle ratio of 0.69

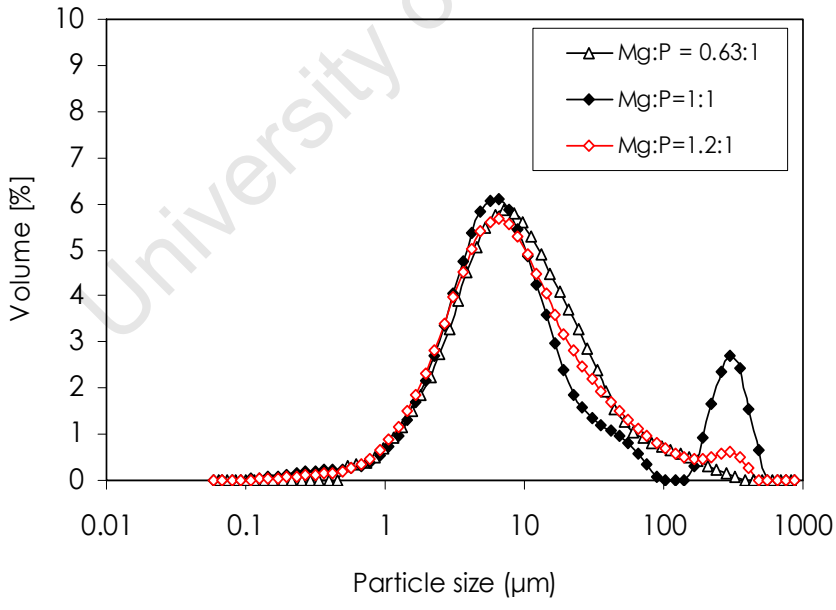

Figure 44: Typical particle size distribution (PSD) in the fluidised bed outlet stream under pH 9 conditions with a recycle ratio of 0.69.

Several workers (Le Corre et al., 2005; Jaffer et al., 2002) have shown that high Mg:P molar ratios limit the precipitation of calcium phosphate. In this study, it is apparent that an

increase in Mg:P molar ratio has no significant effect on calcium conversion as shown in Figure 45. The XRD showed that the dominant solid formed under pH 9 conditions and different Mg:P molar ratios was struvite. However, it is evident that the struvite purity is affected by an increase in Mg:P molar ratio. High purity struvite is achieved at high Mg:P molar ratios and high recycle ratios. The XRD showed that trace amounts of $CaHPO_4.2H_2O$ are formed when the Mg:P molar ratio is 1:1 and the recycle ratio is 0.56. However, the X-ray diffraction (XRD) patterns exhibit a high level of background noise which indicates that the precipitates may contain amorphous compounds. Probably amorphous calcium precipitates. The calcium conversion is approximately constant when Mg:P molar ratio is increased. Consequently, no conclusions can be drawn regarding the effect of increasing Mg:P molar ratio on limiting calcium precipitation.

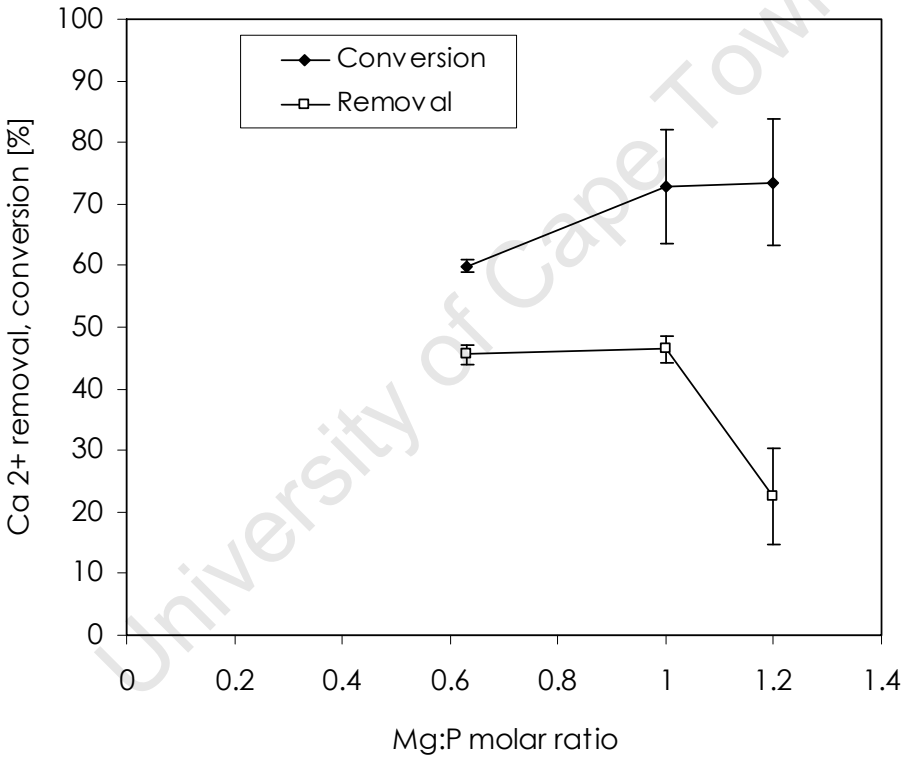

Figure 45: The effect of increasing Mg: P molar ratio on calcium removal and conversion under pH 9 conditions with a recycle ratio of 0.69

Figure 46 shows the removal and conversion when the FBR is operated at a lower recycle flow rate (i.e. RR= 0.56). The PO_4-P conversion for a Mg: P molar ratio of 1:1 and 1.2:1 was approximately 48% and 78% respectively. These conversions are lower than conversions of the system operated at high recycle ratio (i.e. RR= 0.69). An increase in recycle flow rates increases the amount of struvite seed particles recycled back into the FBR. Thus, high mass concentration of struvite particles in the recycle enhances the PO_4-P conversion. This is in

agreement with the previous work by Yoshino and co-workers (2003) which showed that high struvite mass concentration in the recycle increases the kinetics of PO_4-P conversion. This can be explained by the fact that, a large quantity of the struvite particles promotes heterogeneous precipitation and also provides favourable nucleation site for struvite growth (Doyle et al., 2002). However, the effect of PO_4-P conversion enhancement is apparent in the system with very low supersaturation ratios similar to the waste stream treated in this study (Liu et al., 2008).

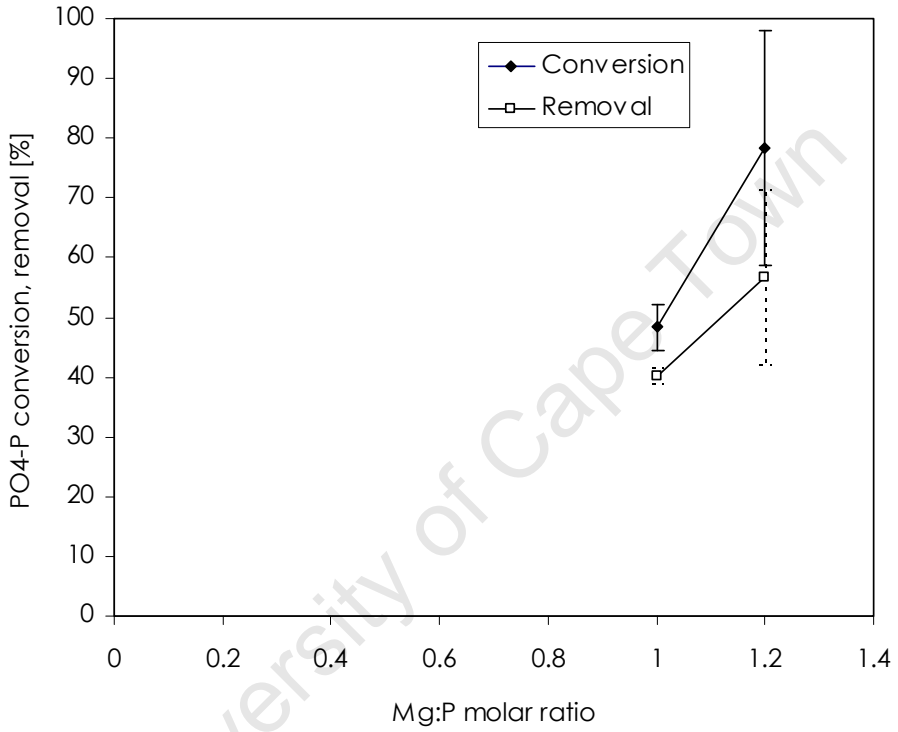

Figure 46: The effect of increasing Mg: P molar ratio on PO_4-P removal and conversion under pH 9 conditions with a recycle ratio of 0.56

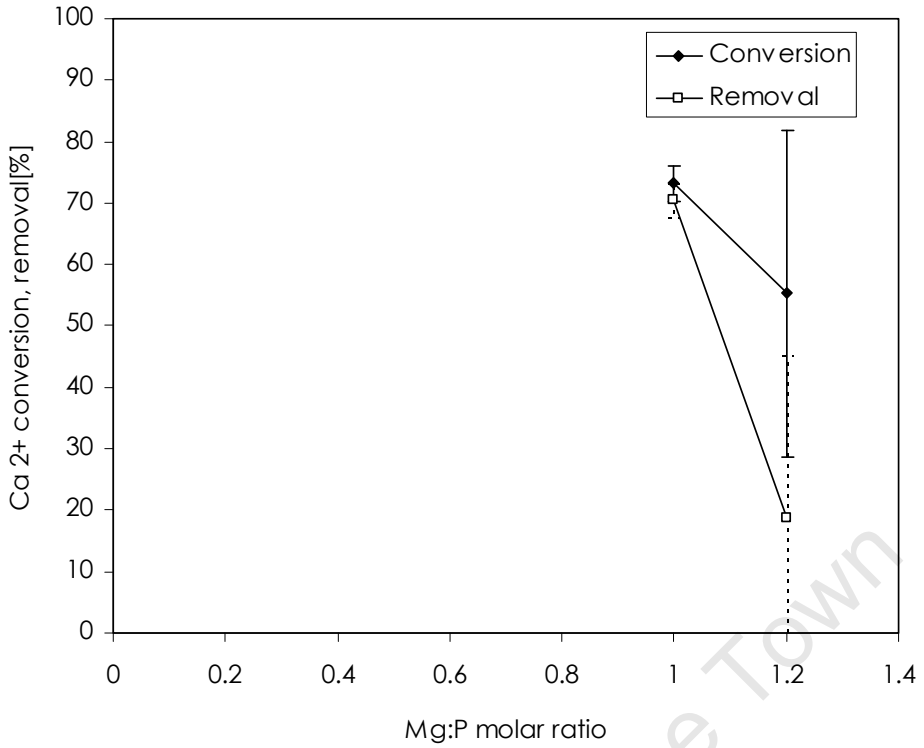

Figure 47: The effect of increasing Mg: P molar ratio on Ca_2^+ removal and conversion under pH 9 conditions with a recycle ratio of 0.56

Several workers have shown that NH_4^+ removal in waste water is primarily through struvite precipitation and NH_3 volatilisation (Uludag-Demirer and Othman, 2009; Liu et al., 2008). The XRD also shows trace amounts of baracite ($(Mg, Fe)_3(PO_4)_2.8H_2O$)) at low Mg:P molar ratios. Baracite ($(Mg,Fe)_3(PO_4)_2.8H_2O$) can be taken as $Mg_{,3}(PO_4)_2.8H_2O$ since the wastewater solution contains no Fe ions. Several workers have shown that $Mg_{,3}(PO_4)_2.8H_2O$ is induced at higher Mg:P molar ratio (Warmadewanthi and Liu., 2008).

A layer of crystals attached on the fluidised bed reactor (FBR) wall was observed during the course of the experimentation. This layer blocked the FBR bypass, as a result the pH control and hydrodynamics in the FBR were affected. Several researchers (Wilsenach et al., 2007; Liu et al., 2008) have observed the layer of crystals precipitating on the walls of the reactor . Doyle et al. (2002) showed that the struvite scaling is dependent on the type of material used. Large amounts of struvite precipitation were observed on the stainless steel stirrer blades whilst this was significantly reduced on blades made of acrylic (Polymethyl methacrylate). However, it was also shown that scaling increases with an increase in the surface roughness because it provides favourable nucleation sites for struvite precipitation. Furthermore, it was shown that scaling rate increases with time because surface roughness increases as struvite particles continue to form on the surface (Doyle et al. 2002). Operating

the FBR at high flow rates prevents cementation of phosphate particles in the reactor. The SEM images show the orthorhombic crystals attached on the quartz seed particles.

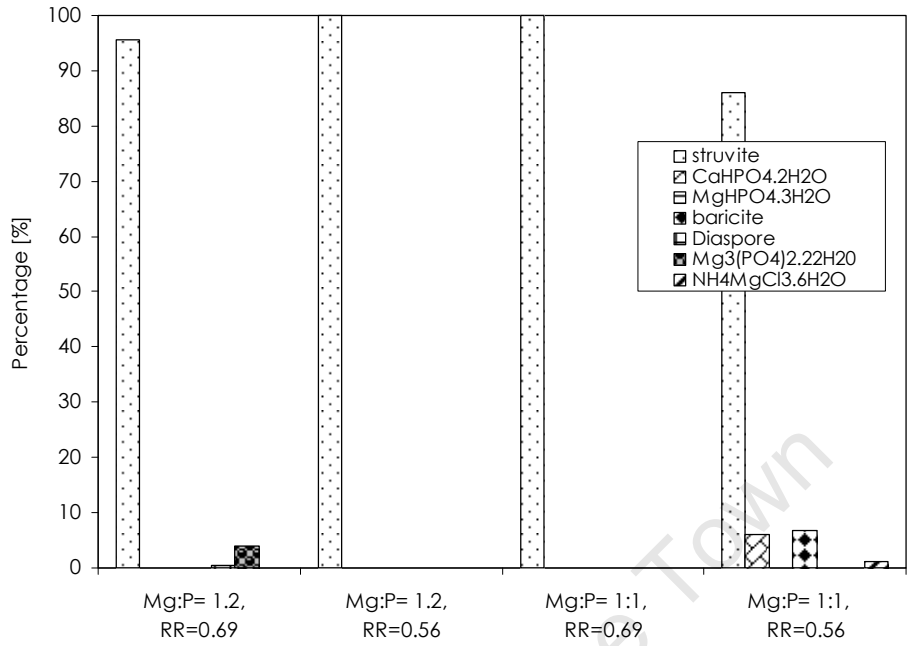

Figure 48: The quantitative XRD results showing the composition of the solids formed under different Mg: P molar ratios and different recycle ratios

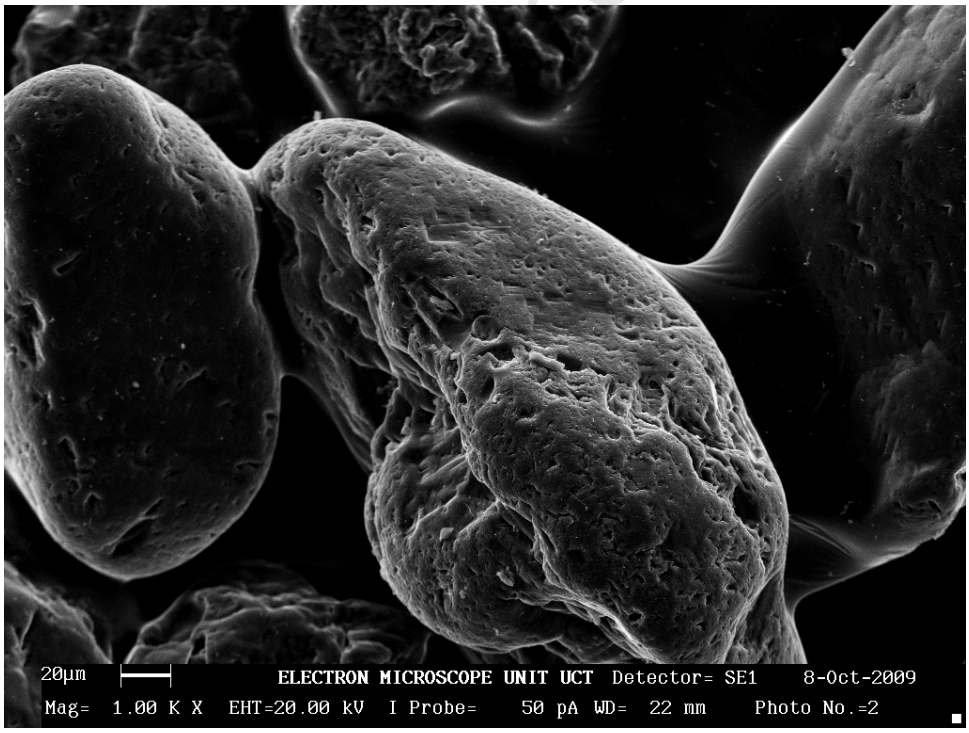

Figure 49: SEM image of the quartz seed particles before the experiment was conducted

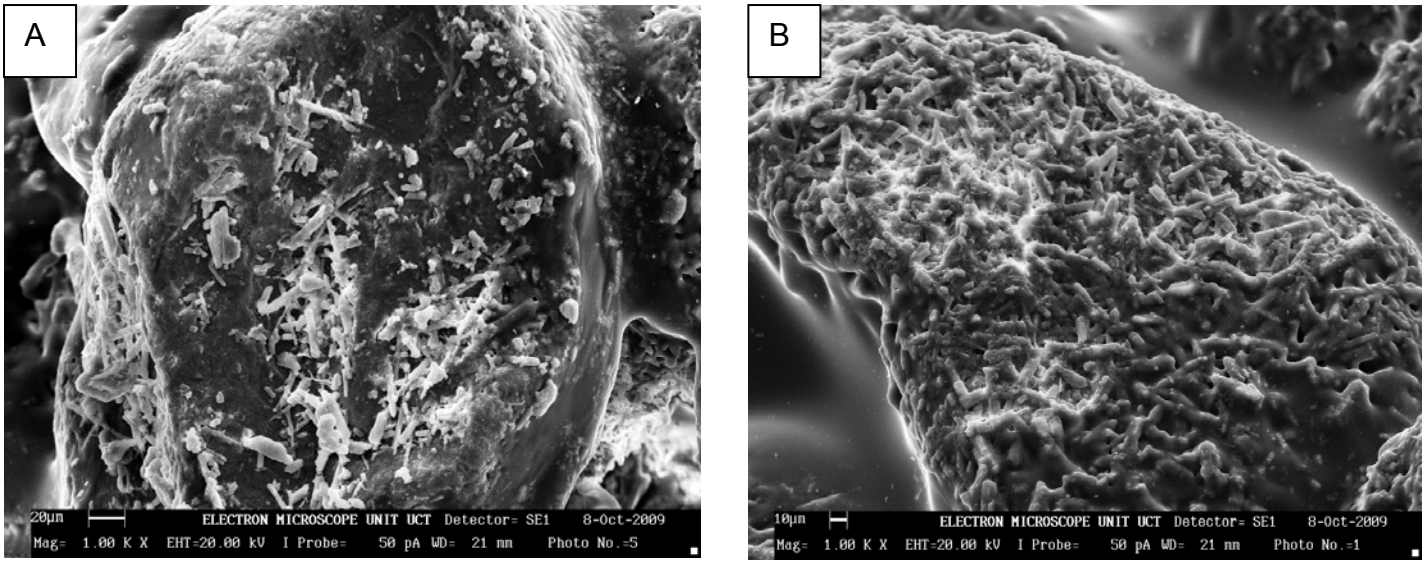

Figure 50: SEM pictures of the seed particles after the experiment under pH 9 conditions. A= Mg: P = 1:1 and RR= 0.69, B = Mg: P = 1:2 and RR= 0.69

6. Conclusions

The preliminary findings from the desktop aqueous chemistry modelling study, bench scale experiments and continuous flow experiments are as follows:

- The pH of the system has a significant effect on phosphate removal due to its influence on the availability of PO_4^{3-}, NH_4^+ and Mg^{2+}. According to the thermodynamic model, phosphates are removed as $Ca_3(PO_4)_2$ and $Mg_3(PO_4)_2.8H_2O$. Phosphate removal as $Mg_3(PO_4)_2.8H_2O$ starts at a pH above 7 with the maximum removal achieved at pH 10. Thereafter, phosphate removal as $Mg_3(PO_4)_3.8H_2O$ drops to zero due to $Mg(OH)_2$ precipitation being favoured at high pH values.
- Moreover, the thermodynamic model and bench scale experiments show that a high NH_4^+: P molar ratio is required to induce struvite precipitation.
- Bench scale experiments showed that, for sample C1, which had PO_4-P and NH_4^+ concentrations of 145mg/L and 65mg/L respectively, the phosphate removed was approximately 30%, 80% and 92% at pH 8, pH 9 and pH 10, respectively. The NH_4^+:P molar ratio in the precipitate decreased to zero because NH_3 formation was favoured at pH 10. The XRD analysis showed that the precipitate was $Mg_3(PO_4)_2.22H_2O$. On the other hand, it was shown that phosphate was removed as struvite under pH 9 conditions for sample C2 which had PO_4-P and NH_4^+ concentrations of 93mg/L and 57mg/L, respectively. The NH_4^+:P molar ratio of sample C1 was 0.99 while the NH_4^+:P molar ratio of sample C2 was 1.35. Thus, high NH_4^+:P molar ratio in the system favours struvite precipitation.
- Fluidized bed reactor experiments showed that high Mg:P molar ratios increased the phosphate removal as a result of the increased Mg^{2+} concentration. However, high Mg: P molar ratios also increased the supersaturation which leads to the formation of many fine particles. There is an increase in overall conversion from 68% to 83 % when the Mg:P molar ratio is increased from 1:1 to 1.2:1. On the other hand, the removal decreased from 45% to 38% when the Mg:P molar ratio is increased from 1:1 to 1.2:1.
- Fluidized bed reactor experiments also showed that high recycle ratios increase the mass concentration of struvite in the system. As a result, PO_4-P conversion was increased because struvite particles provided favourable nucleation sites for struvite formation.

7. Recommendations

1. In order to remove phosphate as struvite it is recommended that the FBR be operated at pH 9 to ensure the optimal availability of NH_4^+, $Mg^{2+}$and PO_4^{3-} ions required for struvite precipitation.

2. Based on the findings that the PO_4-P in sample C1 was removed as $Mg_3(PO_4)_2.22H_2O$ whilst the PO_4-P in sample C2 was removed as struvite and that sample C1 with a NH_4^+:PO_4^{3-} molar ratio of approximately 0.99 whilst sample C2 has NH_4^+:PO_4^{3-} molar ratio of approximately 1.35. Therefore, It is recommended that the NH_4^+:PO_4^{3-} molar ratio be increased in waste water streams that have low NH_4^+ :PO_4^{3-} to ensure that PO_4-P is removed as struvite. Alternatively, the waste water stream that has high NH_4^+: PO_4^{3-} can be mixed with the waste water stream that has low NH_4^+:PO_4^{3-} molar ratio.

3. The FBR should be operated at high recycle ratio to avoid cementation of struvite particles in the reactor. Furthermore, high recycle ratios increase the mass concentration of struvite particles, which provide favourable nucleation sites for struvite formation.

4. More experiments needs to be conducted using struvite seed particles in the fluidized bed reactor instead of quartz particles in order to establish the effect of struvite particles on phosphate removal.

8. References

Ali, M.I. 2007, "Struvite Crystallization in Fed-Batch Pilot Scale and Description of Solution Chemistry of Struvite", *Chemical Engineering Research and Design,* vol. 85, no. 3, pp. 344-356.

Ali, M.I. & Schneider, P.A. 2006, "A fed-batch design approach of struvite system in controlled supersaturation", *Chemical Engineering Science,* vol. 61, no. 12, pp. 3951-3961.

Apha, 1998. Standard Method for the examination of water and wastewater. American Public Health Association/ American Water Works Association/ Water Environment Federation, vol. 20.

Babić-Ivančić, V., Kontrec, J., Brečević, L. & Kralj, D. 2006, "Kinetics of struvite to newberyite transformation in the precipitation system MgCl2–NH4H2PO4–NaOH–H2O", *Water Research,* vol. 40, no. 18, pp. 3447-3455.

Battistoni, P., De Angelis, A., Prisciandaro, M. and others. 2002. P removal from anaerobic supernatants by struvite crystallization: long term validation and process modelling. *Water Research.* 36(8):1927-1938.

Battistoni, P., Fava, G., Pavan, P. and others. 1997. Phosphate removal in anaerobic liquors by struvite crystallization without addition of chemicals: Preliminary results. *Water research.* 31(11):2925-2929.

Bouropoulos, N.C. & Koutsoukos, P.G. 2000, "Spontaneous precipitation of struvite from aqueous solutions", *Journal of Crystal Growth,* vol. 213, no. 3-4, pp. 381-388.

Çelen, I., Buchanan, J.R., Burns, R.T., Bruce Robinson, R. & Raj Raman, D. 2007, "Using a chemical equilibrium model to predict amendments required to precipitate phosphorus as struvite in liquid swine manure", *Water Research,* vol. 41, no. 8, pp. 1689-1696.

Costodes, V.C.T. & Lewis, A.E. 2006. Reactive crystallization of nickel hydroxy-carbonate in fluidized-bed reactor: Fines production and column design. *Chemical Engineering Science.* 61(5):1377-1385.

de-Bashan, L.E. & Bashan, Y., 2004. Recent advances in removing phosphorus from wastewater and its future use as fertilizer (1997–2003). Water Research, vol 38, no. 19, pp. 4222-4246

Doyle, J.D., Philp, R., Churchley, J. & Parsons, S.A. 2000, "Analysis of Struvite Precipitation in Real and Synthetic Liquors", *Process Safety and Environmental Protection,* vol. 78, no. 6, pp. 480-488.

Doyle, J.D. & Parsons, S.A. 2002, "Struvite formation, control and recovery", *Water Research,* vol. 36, no. 16, pp. 3925-3940.

Hirasawa, I., Shimamura, K. & Suzuki, Y., 2008 "Recovery of phosphorus in the wastewater as resources based on crystallization engineering", .

Jaffer, Y., Clark, T.A., Pearce, P. & Parsons, S.A. 2002, "Potential phosphorus recovery by struvite formation", *Water Research,* vol. 36, no. 7, pp. 1834-1842.

Jones, A.G. (2002) Crystallisation process systems, Butterworth-Heinemann, Boston, Oxford

Kim, D., Ryu, H., Kim, M., Kim, J. & Lee, S. 2007, "Enhancing struvite precipitation potential for ammonia nitrogen removal in municipal landfill leachate", *Journal of hazardous materials,* vol. 146, no. 1-2, pp. 81-85.

Karpinski, P.H., Wey, J.S., 2002. *Handbook of Industrial Crystallization*, 2nd ed., *Chapter 6 precipitation processes*. Butterworth-Heinemann Ltd., Wolburn, MA, pp. 141–159.

Le Corre, K.S., Valsami-Jones, E., Hobbs, P., Jefferson, B. & Parsons, S.A. 2007, "Agglomeration of struvite crystals", *Water Research,* vol. 41, no. 2, pp. 419-425.

Le Corre, K.S., Valsami-Jones, E., Hobbs, P. & Parsons, S.A. 2005, "Impact of calcium on struvite crystal size, shape and purity", *Journal of Crystal Growth,* vol. 283, no. 3-4, pp. 514-522.

Lee, S.I., Weon, S.Y., Lee, C.W. & Koopman, B. 2003, "Removal of nitrogen and phosphate from wastewater by addition of bittern", *Chemosphere,* vol. 51, no. 4, pp. 265-271.

Liu, Z., Zhao, Q., Lee, D. & Yang, N. 2008, "Enhancing phosphorus recovery by a new internal recycle seeding MAP reactor", *Bioresource technology,* vol. 99, no. 14, pp. 6488-6493.

Mijangos, F., Kamel, M., Lesmes, G. & Muraviev, D.N. 2004, "Synthesis of struvite by ion exchange isothermal supersaturation technique", *Reactive and Functional Polymers,* vol. 60, pp. 151-161.

Musvoto, E.V., Wentzel, M. & Ekama, G.A., 2000, "Integrated chemical-physical processes modelling-II. Simulating aeration treatment of anaerobic digester supernatants. Water Res. 34 , 1857-1867

Nelson, N.O., Mikkelsen, R.L. & Hesterberg, D.L. 2003, "Struvite precipitation in anaerobic swine lagoon liquid: effect of pH and Mg:P ratio and determination of rate constant", *Bioresource Technology,* vol. 89, no. 3, pp. 229-236.

Nielsen, A.E. (1964) Kinetics of precipitation, Pergamon, Oxford

Ohlinger, K.N., Young, T.M. & Schroeder, E.D. 1998, "Predicting struvite formation in digestion", *Water Research,* vol. 32, no. 12, pp. 3607-3614.

OLI Systems Inc, 2008. OLI Stream Analyser, version 2.0.57, Morris Plains, New Jersey, USA

Pastor, L., Mangin, D., Barat, R. & Seco, A., 2008. A pilot-scale study of struvite precipitation in a stirred tank: Conditions influencing the process. Bioresource Technology, doi:10.1016/j.biortech.2007.12.003

Richardson, J.F., Harker, J.H. and Backhust, J.R., 2002, Coulson & Richardson's chemical engineering, particle technology and separation process, 5th ed., vol 2., chapter 6, fluidization, Butterworth-Heinemann Ltd., pp.291-365

Ryu, H., Kim, D. & Lee, S. 2008, "Application of struvite precipitation in treating ammonium nitrogen from semiconductor wastewater", *Journal of Hazardous Materials,* vol. In Press, Corrected Proof.

Seckler, M.M., Bruinsma, O.S.L. & Van Rosmalen, G.M. 1996, "Phosphate removal in a fluidized bed—I. Identification of physical processes", *Water Research,* vol. 30, no. 7, pp. 1585-1588.

Shu, L., Schneider, P., Jegatheesan, V. & Johnson, J., 2006. An economic evaluation of phosphorus recovery as struvite from digester supernatant. Bioresource Technology, vol 97, no. 17, pp. 2211-2216.

Söhnel, O. and Garside, J. (1992). Precipitation: Basic principles and applications, Butterworth-Heinemann, Oxford,

Stratful, I., Scrimshaw, M.D. & Lester, J.N. 2001, "Conditions influencing the precipitation of magnesium ammonium phosphate", *Water Research,* vol. 35, no. 17, pp. 4191-4199.

Türker, M. & Çelen, I. 2007, "Removal of ammonia as struvite from anaerobic digester effluents and recycling of magnesium and phosphate", *Bioresource technology,* vol. 98, no. 8, pp. 1529-1534.

Uludag-Demirer, S., Demirer, G.N. & Chen, S. 2005, "Ammonia removal from anaerobically digested dairy manure by struvite precipitation", *Process Biochemistry,* vol. 40, no. 12, pp. 3667-3674.

Uludag-Demirer, S. & Othman, M. 2009, "Removal of ammonium and phosphate from the supernatant of anaerobically digested waste activated sludge by chemical precipitation", *Bioresource technology,* vol. 100, no. 13, pp. 3236-3244.

van Rensburg, P., Musvoto, E.V., Wentzel, M.C. & Ekama, G.A., 2003. Modelling multiple mineral precipitation in anaerobic digester liquor. Water Research, vol 37, no.13, pp. 3087-3097.

Wang, P., Anderko, A., Springer, R.D. & Lencka, M.M. 2008, "Speciation and phase behavior in mixed solvent electrolyte solutions: Thermodynamic modelling", *17th international symposium on industrial crystallization,* vol. 1, pp. 471-478.

Warmadewanthi & Liu, J.C., 2008, "Recovery of Phosphate, Ammonium as Struvite from Semiconductor Wastewater", *Separation and Purification Technology,* vol. In Press, Accepted Manuscript.

Wilsenach, J.A., Schuurbiers, C.A.H. & van Loosdrecht, M.C.M. 2007, "Phosphate and potassium recovery from source separated urine through struvite precipitation", Water research, vol. 41, no. 2, pp. 458-466.

Yoshino, M., Yao, M., Tsuno, H. & Somiya, I. 2003, "Removal and recovery of phosphate and ammonium as struvite from supernatant in anerobic digestion", *Water Science and technology,* vol. 48, no. 1, pp. pp.171-178.

9. Appendices

Appendix A: Analytical procedures and methods

1. Procedure for the determining of the PO_4-P concentration (Vanadomolybdophosphoric acid colorimetric method)

The method of determining the PO_4-P concentration was based on the following principle: In a dilute orthophosphate solution, ammonium molybdate reacts under acid solution to form a molydophosphoric acid which forms a yellow vanadolymolybdophosphoric acid in the presence of vanadium. The intensity of the yellow colour is proportional to phosphate concentration (Apha, 1998).

Reagents and procedure (Lakay et al., 2000)

1. Vanadomolybdate reagent

Solution A: 20g of ammonium molybdate tetradrate was dissolved in 250 ml distilled water.

Solution B: 1g ammonium metavanadate was dissolved in 40 ml concentrated nitric acid (65%) and 200 ml distilled water.

Solution A and solution B were mixed, and 100 ml concentrated nitric acid (65%) was added. The mixed solutions were diluted to 1000ml with distilled water.

2. Standard PO_4-P solutions

Standard PO_4-P solutions of 5mg/l, 10 mg/l, 15 mg/l, 20 mg/l and 25 mg/l were prepared by adding anhydrous KH_2PO_4 to distilled water.

3. Sulphuric acid solution

6.1 ml of concentrated sulphuric acid (98%) was added to about 500ml of distilled water. After approximately 5 minutes and the solution was diluted to 1000ml with distilled water.

4. Potassium persulphate solution

3 g of potassium persulphate was dissolved in 100 ml of distilled water.

PO_4-P calibration curve

5ml of PO_4-P solution was added to 5ml of Vanadomolybdate reagent. The absorbance was measured using the spectrophotometer at wavelength 470µm.

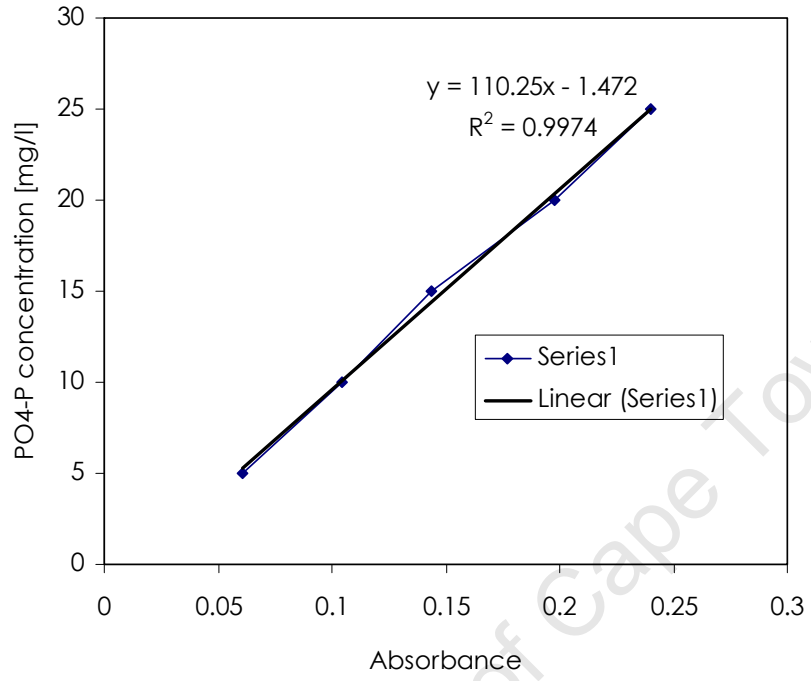

Figure 51: Calibration curve of the spectrophotometer at wavelength 470 µm.

The equation obtained from the calibration curve was used to measure the concentration in the PO_4-P [mg/l] in the waste water. The waste water samples were diluted accordingly to ensure that the PO_4-P concentration is below 25 mg/L.

Total phosphate

Total phosphate was obtained by heating a 20ml sample with 5ml of sulphuric acid and 5 ml potassium sulphate solution for 20 minutes at 90^{o}C water bath.

The calibration curve equation obtained was y = 146.09x + 0.8634 and the corresponding R^2 correlation= 0.9267

Possible interference

Ions that will interfere if their concentrations are greater than 1000 mg/L are Al^{3+},Fe^{3+},Mg^{2+},Ca^{2+},NH_4^+, Na^+,K^+,CO_3^{2-} and SO_4^{2-} (Apha , 1998). The concentrations of these ions in Tswane municipality waste stream were below 1000 mg/L.

Reference:

1. Apha Awwa wef 1998, "Standard Method for the examination of water and wastewater",*American public Health association/ American water works association/ water environment federation,* vol. 20.
2. Lakay, M.T., Wentzel, M.C. and Ekama, G.A, 2000, " Laboratory procedures-wastewater treatment laboratory" University of Cape Town department of civil engineering.

Appendix B: Reproducibility of the experimental results

The fluidized bed reactor experiments were repeated 3 times under the different experimental conditions investigated herein. The graphs below show the results obtained and that the results were reproducible. The results presented in this thesis are an average of the results obtained when the fluidized bed reactor is at steady state. It is apparent that steady state was reached within 4 hours. The pH at the bottom of the reactor was kept constant at pH 9. When the pH in the FBR was not at the set point the PO_4-P removal varied slightly. The pH deviated from the set point by ± 0.2. Consequently, the concentrations for the 3 experiments were slightly different because the phosphate removal is highly pH dependent.

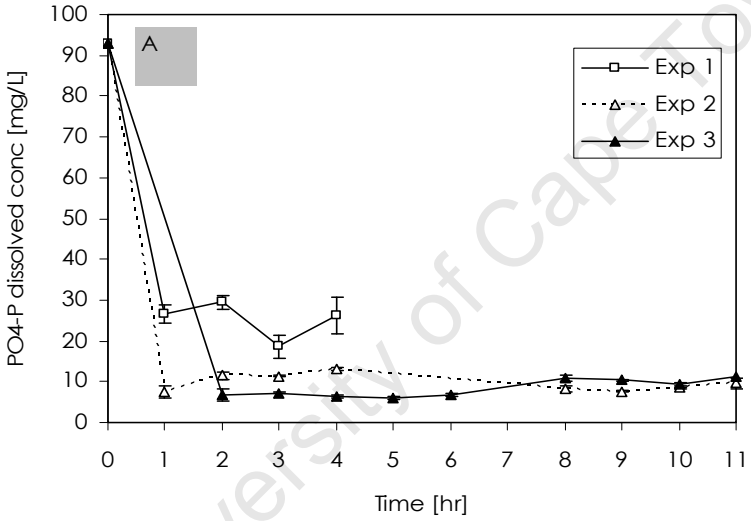

Figure 52: PO4-P concentration in the FBR outlet stream when the initial Mg: P = 1.2 and the recycle ratio = 0.69 under pH 9 conditions.

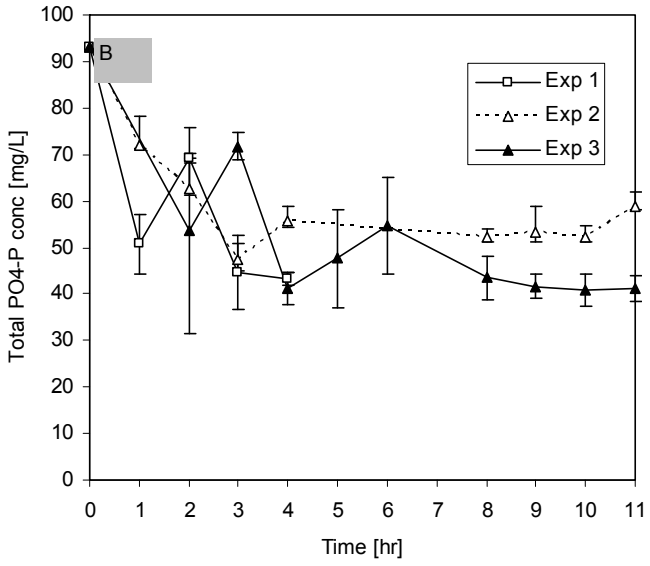

Figure 53: Total PO_4-P concentration in the FBR outlet stream when the initial Mg: P = 1.2 and the recycle ratio = 0.69 under pH 9 conditions.

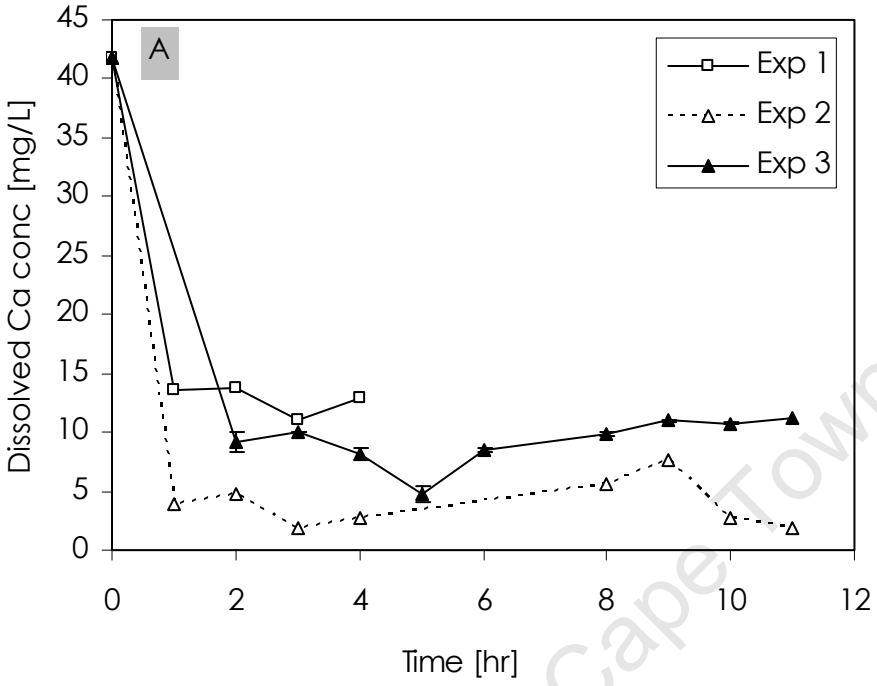

Figure 54: Dissolved Ca^{2+} concentration in the FBR outlet stream when the initial Mg:P= 1.2 and the recycle ratio = 0.69 under pH 9 conditions

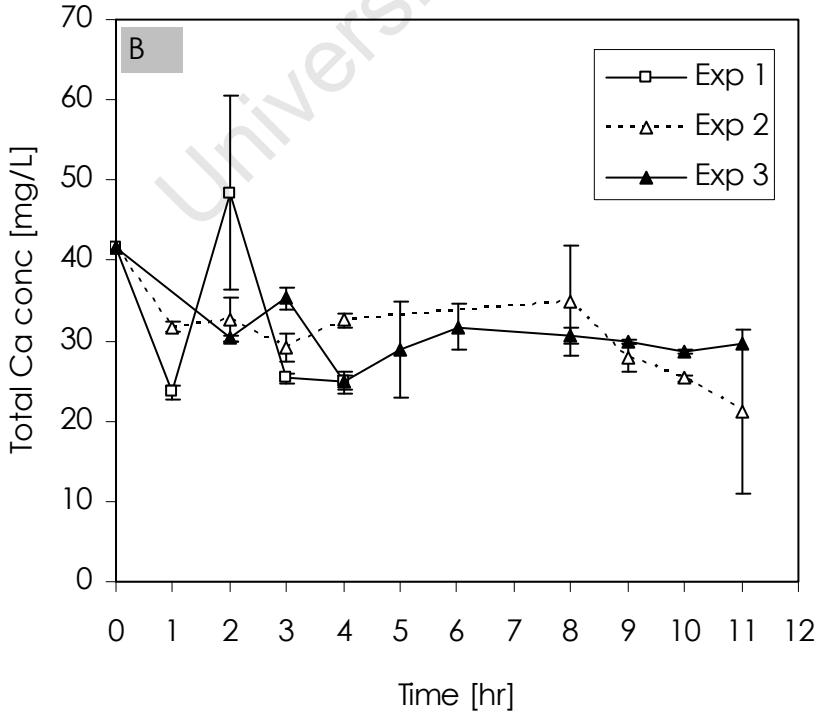

Figure 55: Total Ca^{2+} concentration in the FBR outlet stream when the initial Mg:P= 1.2 and the recycle ratio = 0.69 under pH 9 conditions.

Appendix C: X-ray diffraction (XRD) of bench scale experiments for selected samples showing the reference patterns

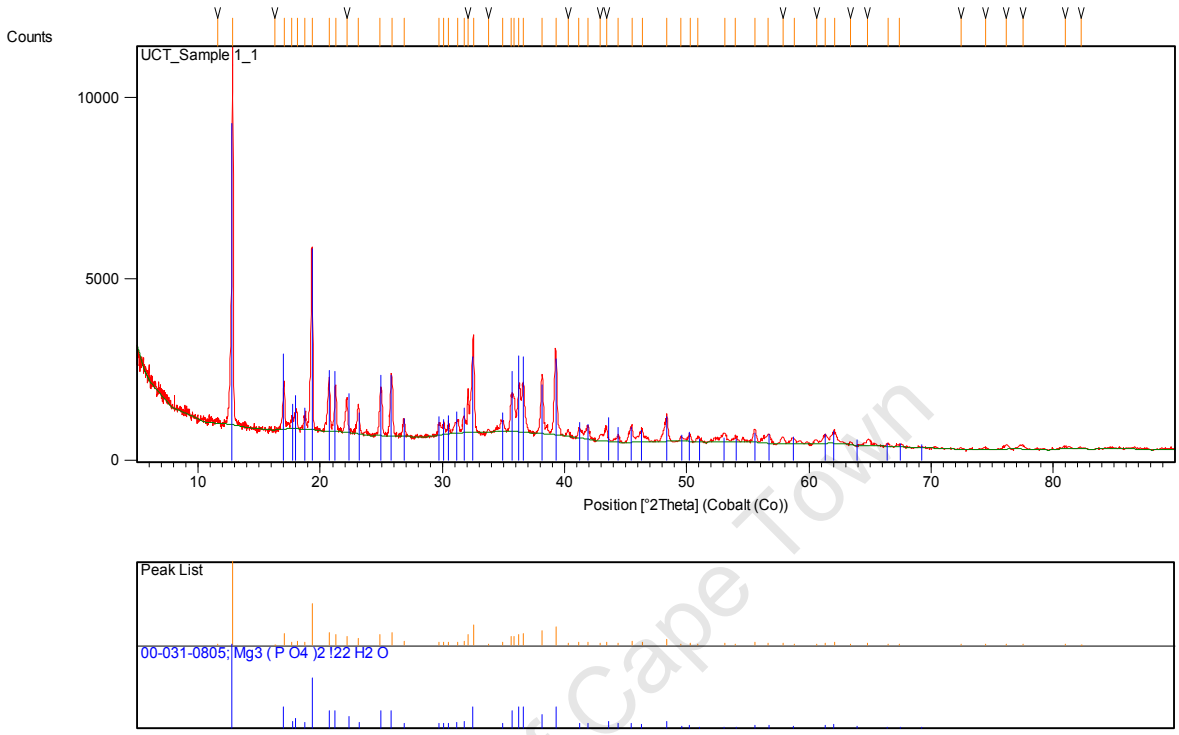

Figure 56: Typical X-ray diffraction (XRD) pattern precipitate formed from sample C1 when the Mg: P = 1: 1 and pH =9 showing the reference pattern of $Mg_3(PO_4)_2.22H_2O$

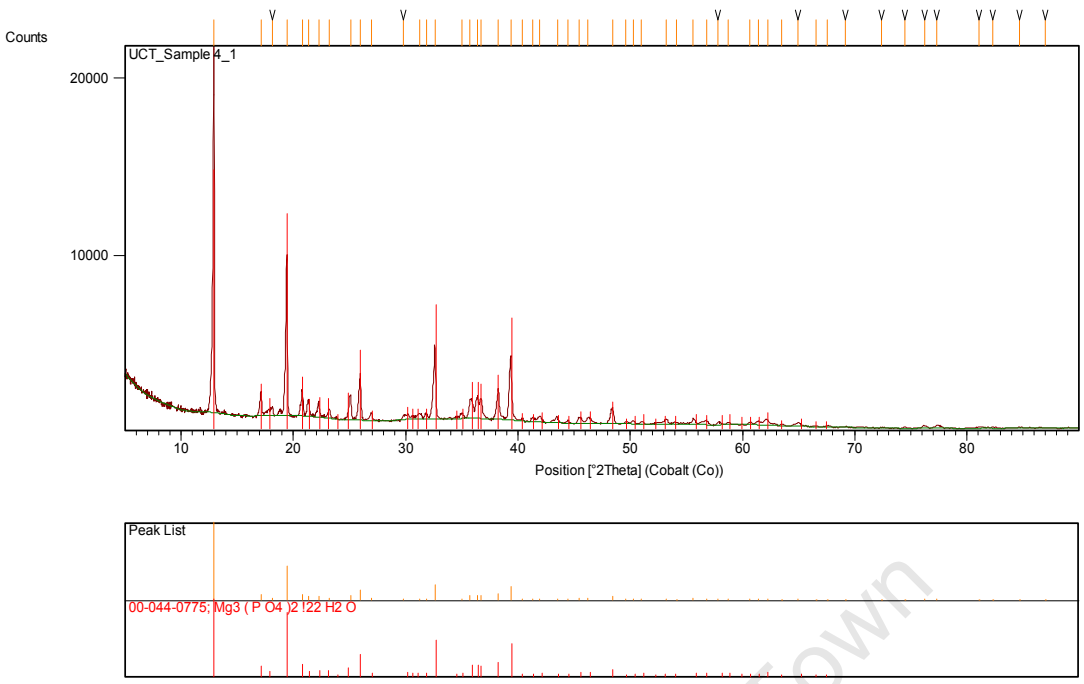

Figure 57: Typical X-ray diffraction (XRD) pattern precipitate formed from sample C1 when the Mg: P = 1: 1 and pH =10 showing the reference pattern of $Mg_3(PO_4)_2.22H_2O$.

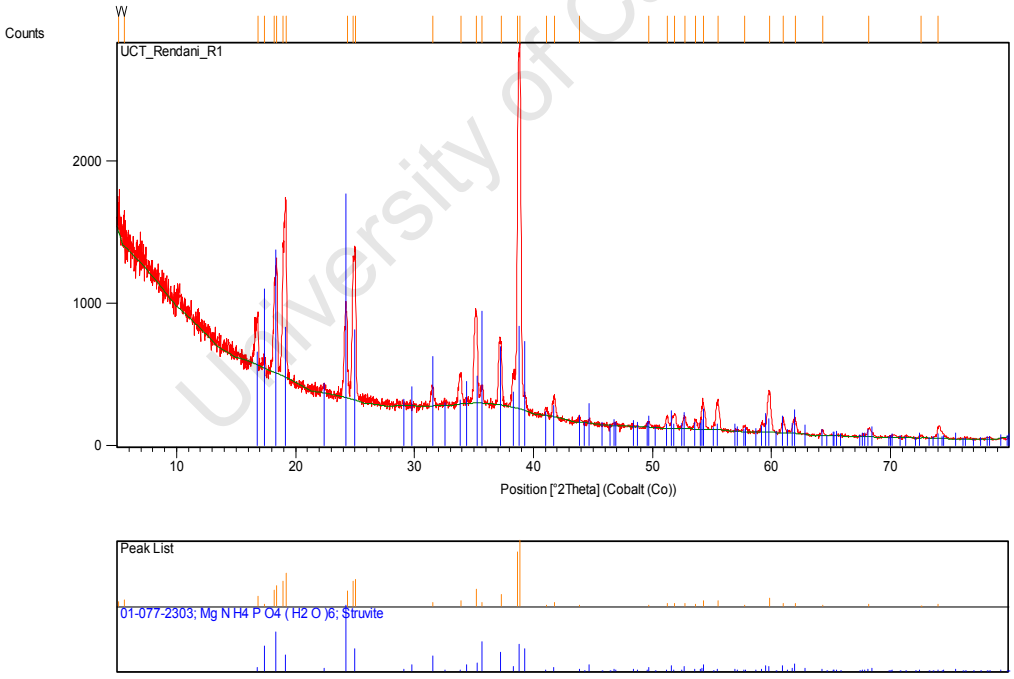

Figure 58: Typical X-ray diffraction (XRD) pattern of precipitate formed from sample C2 when the Mg: P = 1: 1 and pH =9 showing the reference pattern of $MgNH_4PO_4.6H_2O$ (struvite).

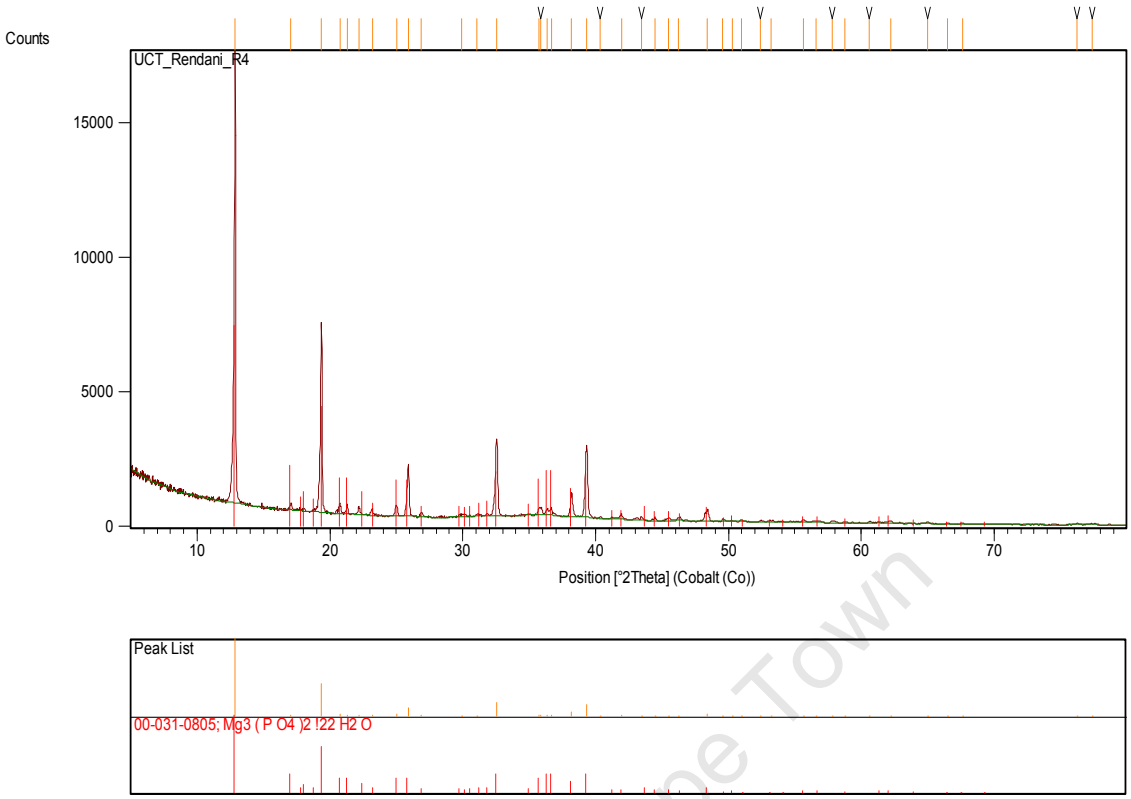

Figure 59: Typical X-ray diffraction (XRD) pattern of the precipitate formed from sample C2 when the Mg: P = 1: 1 and pH =10 showing the reference pattern of $Mg_3(PO_4)_2.22H_2O$.

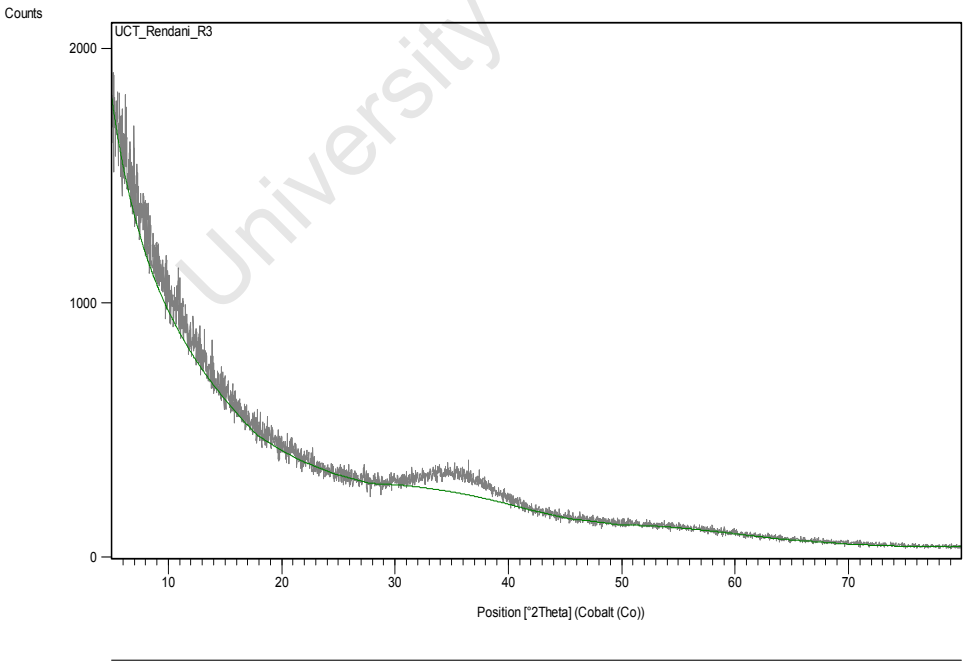

Figure 60: Typical XRD pattern precipitate formed from sample C2 when Ca:P molar ratio was 0.85 and under 9 conditions showing that no crystalline compounds are formed.

Appendix D: X-ray diffraction (XRD) patterns of the precipitate formed in the fluidized bed reactor experiments for selected samples showing the reference patterns.

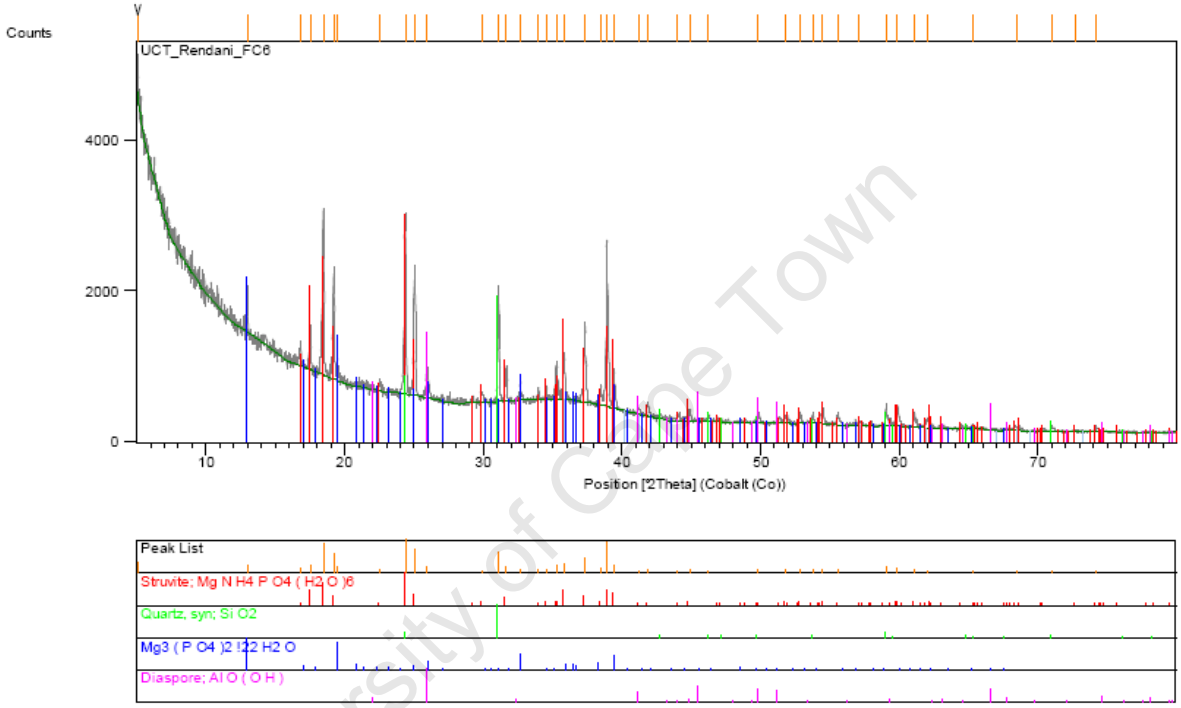

Figure 61: Typical XRD pattern of precipitate formed in the fluidized bed reactor under pH 9 condition, Mg:P molar ratio of 1.2 and the recycle ratio of 0.69.

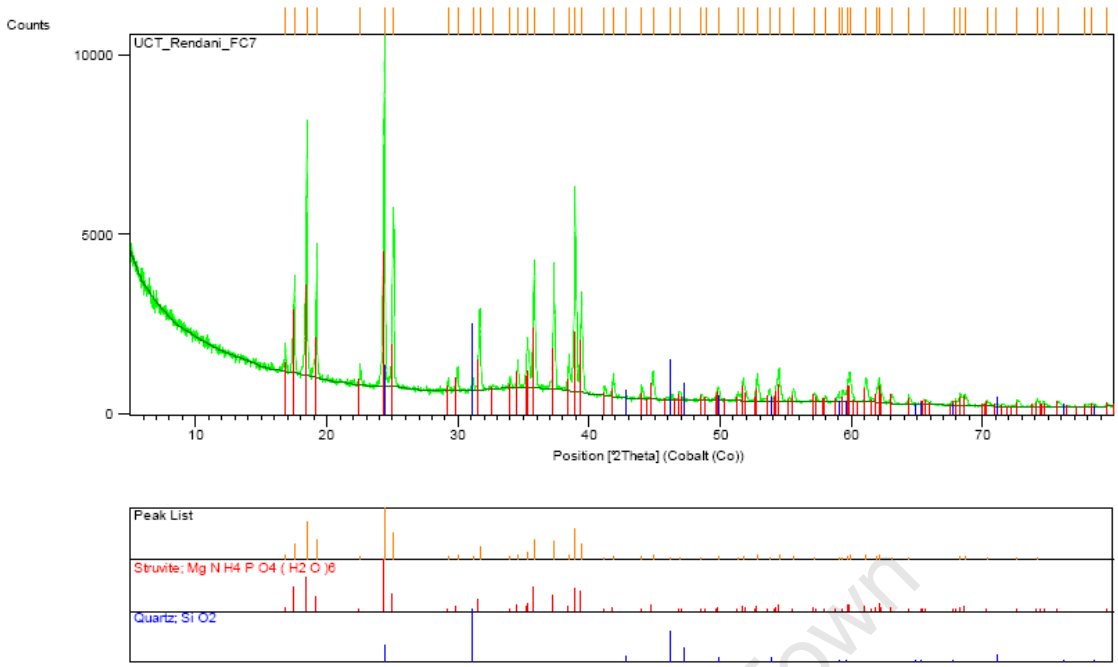

Figure 62: Typical XRD pattern of precipitate formed in the fluidized bed reactor under pH 9 condition, Mg:P molar ratio of 1:1 and the recycle ratio of 0.69.

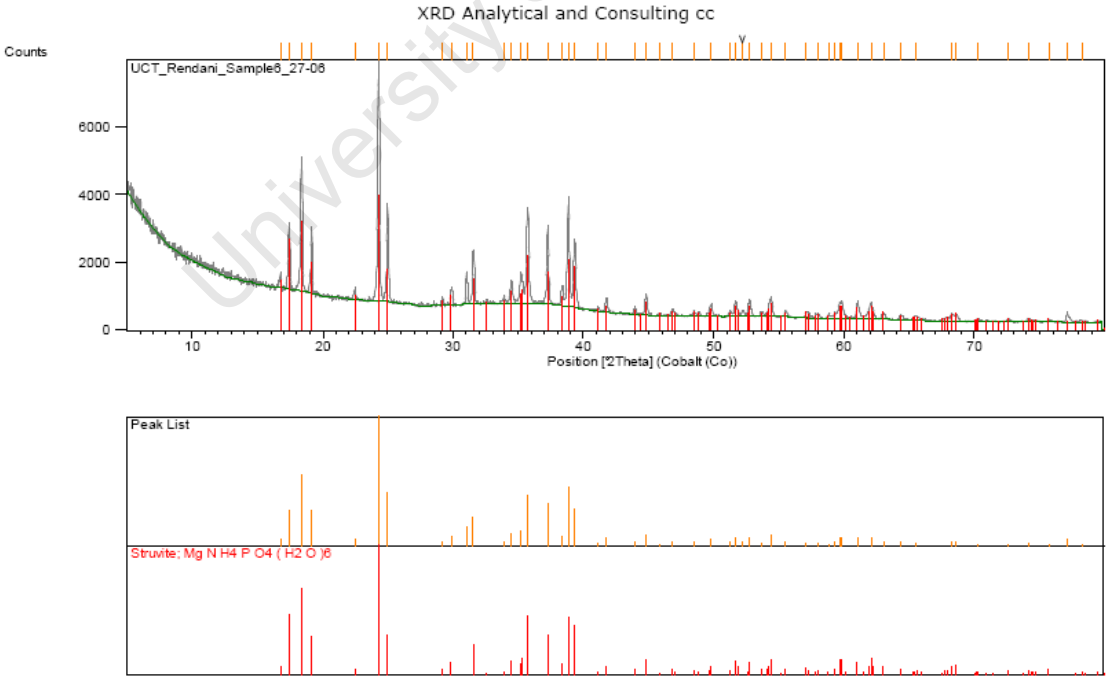

Figure 63: Typical XRD pattern of precipitate formed in the fluidized bed reactor under pH 9 conditions, Mg:P molar ratio of 1.2:1 and the recycle ratio of 0.56.

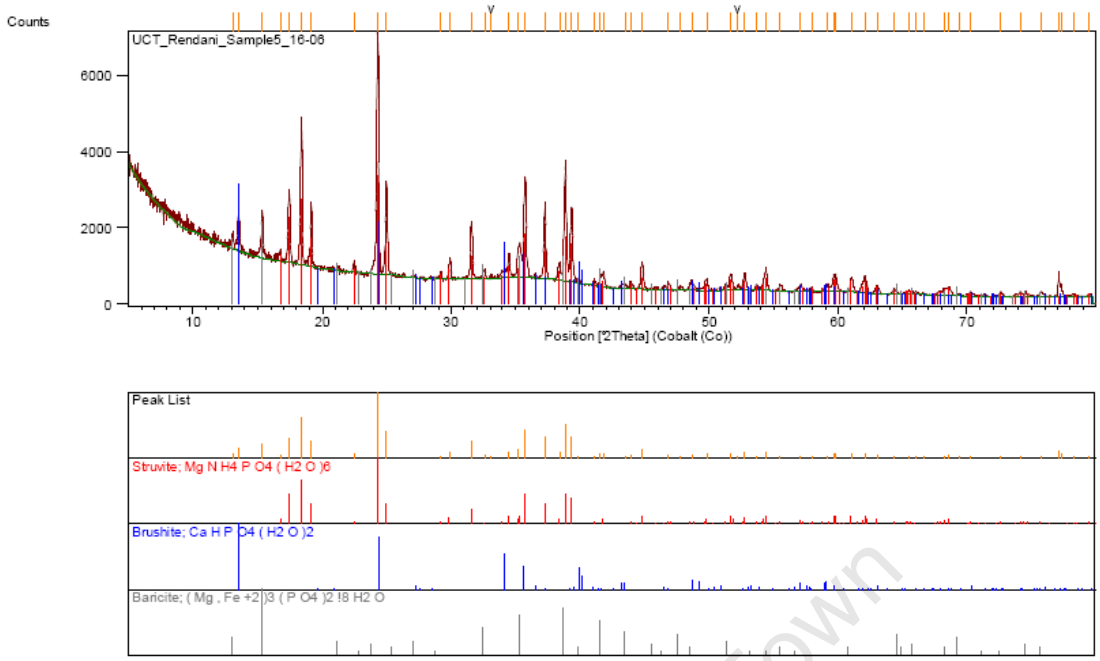

Figure 64: Typical XRD pattern of precipitate formed in the fluidized bed reactor under pH 9 conditions, Mg:P molar ratio of 1:1 and the recycle ratio of 0.56.